SLL 84-U-091

UNCLASSIFIED ⟶ Prater

NBS TECHNICAL NOTE **993**

U.S. DEPARTMENT OF COMMERCE / National Bureau of Standards

Optical Materials
Characterization
Final Technical Report
February 1, 1978-
September 30, 1978

19980309 197

UNCLASSIFIED

U 5160

NATIONAL BUREAU OF STANDARDS

The National Bureau of Standards[1] was established by an act of Congress March 3, 1901. The Bureau's overall goal is to strengthen and advance the Nation's science and technology and facilitate their effective application for public benefit. To this end, the Bureau conducts research and provides: (1) a basis for the Nation's physical measurement system, (2) scientific and technological services for industry and government, (3) a technical basis for equity in trade, and (4) technical services to promote public safety. The Bureau's technical work is performed by the National Measurement Laboratory, the National Engineering Laboratory, and the Institute for Computer Sciences and Technology.

THE NATIONAL MEASUREMENT LABORATORY provides the national system of physical and chemical and materials measurement; coordinates the system with measurement systems of other nations and furnishes essential services leading to accurate and uniform physical and chemical measurement throughout the Nation's scientific community, industry, and commerce; conducts materials research leading to improved methods of measurement, standards, and data on the properties of materials needed by industry, commerce, educational institutions, and Government; provides advisory and research services to other Government Agencies; develops, produces, and distributes Standard Reference Materials; and provides calibration services. The Laboratory consists of the following centers:

Absolute Physical Quantities[2] — Radiation Research — Thermodynamics and Molecular Science — Analytical Chemistry — Materials Science.

THE NATIONAL ENGINEERING LABORATORY provides technology and technical services to users in the public and private sectors to address national needs and to solve national problems in the public interest; conducts research in engineering and applied science in support of objectives in these efforts; builds and maintains competence in the necessary disciplines required to carry out this research and technical service; develops engineering data and measurement capabilities; provides engineering measurement traceability services; develops test methods and proposes engineering standards and code changes; develops and proposes new engineering practices; and develops and improves mechanisms to transfer results of its research to the utlimate user. The Laboratory consists of the following centers:

Applied Mathematics — Electronics and Electrical Engineering[2] — Mechanical Engineering and Process Technology[2] — Building Technology — Fire Research — Consumer Product Technology — Field Methods.

THE INSTITUTE FOR COMPUTER SCIENCES AND TECHNOLOGY conducts research and provides scientific and technical services to aid Federal Agencies in the selection, acquisition, application, and use of computer technology to improve effectiveness and economy in Government operations in accordance with Public Law 89-306 (40 U.S.C. 759), relevant Executive Orders, and other directives; carries out this mission by managing the Federal Information Processing Standards Program, developing Federal ADP standards guidelines, and managing Federal participation in ADP voluntary standardization activities; provides scientific and technological advisory services and assistance to Federal Agencies; and provides the technical foundation for computer-related policies of the Federal Government. The Institute consists of the following divisions:

Systems and Software — Computer Systems Engineering — Information Technology.

[1]Headquarters and Laboratories at Gaithersburg, Maryland, unless otherwise noted; mailing address Washington,D.C. 20234.
[2]Some divisions within the center are located at Boulder, Colorado, 80303.

The National Bureau of Standards was reorganized, effective April 9, 1978.

Optical Materials Characterization
Final Technical Report
February 1, 1978-September 30, 1978

Albert Feldman, Deane Horowitz,
Roy M. Waxler, and Marilyn J. Dodge

Center for Materials Science
National Measurement Laboratory
National Bureau of Standards
Washington, D.C. 20234

National Bureau of Standards Technical Note 993

Nat. Bur. Stand. (U.S.), Tech. Note 993, 71 pages (Feb. 1979)

CODEN: NBTNAE

U.S. GOVERNMENT PRINTING OFFICE

WASHINGTON: 1979

OPTICAL MATERIALS CHARACTERIZATION

Albert Feldman, Deane Horowitz, Roy M. Waxler, and Marilyn J. Dodge

Ceramics, Glass and Solid State Science Division
Center for Materials Science
National Bureau of Standards

TABLE OF CONTENTS   PAGE

Optical Materials Characterization

Abstract

Data obtained as part of the Optical Materials Characterization Program are summarized in this report. Room temperature values of refractive index as a function of wavelength are presented for the following materials: commercially grown KCl, reactive atmosphere processed (RAP) KCl, KCl nominally doped with 1.5% KI, hot forged CaF_2, fusion cast CaF_2, CaF_2 doped with Er (0.001% to 3% Er), SrF_2, chemical vapor deposited (CVD) ZnSe (2 specimens), and ZnS (CVD, 2 specimens). Data for the thermo-optic constant (dn/dT) and the linear thermal expansion coefficient are given for the following materials over the temperature range −180 °C to 200 °C: Al_2O_3, BaF_2, CaF_2, CdF_2, KBr, KCl, LiF, MgF_2, NaCl, NaF, SrF_2, ZnS (CVD), and ZnSe (CVD). The piezo-optic constants of the following materials are presented: As_2S_3 glass, CaF_2, BaF_2, Ge, KCl, fused SiO_2, SrF_2, a chalcogenide glass (Ge 33%, As 12%, Se 55%) and ZnSe (CVD).

Optical Materials Characterization

1.   Technical Report Summary

1.1 Technical Problem

Windows subjected to high-average-power laser radiation will undergo optical and mechanical distortion due to absorptive heating. If the distortion becomes sufficiently severe, the windows become unusable. Theoretical calculations of optical distortion in laser windows depend on the following material parameters; absorption coefficient, refractive index, the thermo-optic constant (change of index with temperature), linear thermal expansion coefficient, stress-optical constants, elastic compliances, specific heat, thermal conductivity and density. Our program has been established to measure refractive indices, thermo-optic constants, piezo-optic constants, elastic compliances, and linear thermal expansion coefficients of candidate laser window materials.

1.2 General Methodology

Laboratory experiments are conducted for measuring refractive indices, thermo-optic constants, piezo-optic constants, elastic compliances and linear thermal expansion coefficients.

The refractive indices of prismatic specimens are measured on precision spectrometers by the method of minimum deviation. Two spectrometers are used. One instrument, which uses glass optics, is used for measuring refractive indices in the visible with an accuracy of several parts in 10^6. The other instrument, which uses mirror optics, is used for measuring refractive indices in the ultraviolet and the infrared to an accuracy of several parts in 10^5. Using both spectrometers we can measure refractive indices over the spectral region 0.2 µm to 50 µm.

We measure the linear thermal expansion coefficient, α, by the method of Fizeau interferometry. The interferometer consists of a specially prepared specimen which separates two flat plates. Interference fringes are observed due to reflections of HeNe laser radiation at 0.6328 µm from the plate surfaces in contact with the specimen. We obtain α by measuring the shift of these interference fringes as a function of temperature. We can measure α from -180 °C to 800 °C.

The thermo-optic constant, dn/dT, is measured by two methods. In the first method, we measure the refractive index with the precision spectrometers at two temperatures, 20 °C and 30 °C, by varying the temperature of the laboratory. This provides us with a measure of dn/dT near room temperature. In the second method, which may be used for measuring dn/dT from -180 °C to 800 °C, we obtain dn/dT from a knowledge of the expansion coefficient and by measuring the shift of Fizeau fringes in a heated specimen as a function of temperature. The Fizeau fringes are due to interferences between reflections from the front and back surfaces of the specimens. Measurements are made with discrete spectral sources, such as lasers or spectral lamps, in the infrared, the visible, and the ultraviolet.

We measure piezo-optic constants and elastic compliances using a combination of Twyman-Green and Fizeau interferometers. The coefficients for piezo-birefringence are measured by polarimetric techniques. From the shift of fringes in specimens subjected to uniaxial or hydrostatic compression, we obtain the data necessary for determining all the piezo-optic constants and elastic compliances. The measurement are made with discrete spectral sources.

In materials with small piezo-optic constants or in materials that cannot withstand large stresses, we use interferometers designed to measure fractional fringe shifts. At 10.6 µm a modified Twyman-Green interferometer, which has a sensitivity of 0.01 λ, is used. At 632.8 nm, a modified Dyson interferometer, which has a sensitivity of 0.002 λ, is used. When using these interferometers to measure piezo-optic constants we must know the elastic constants of the material under test.

2

1.3 Technical Results

The purpose of this report is to collect in one publication all the data obtained under the Optical Materials Characterization Program. In addition to data found in our previous reports, we present data not yet reported. The data are tabulated in Section 2.9.

Section 2.1 discusses the measurement of refractive index by the method of minimum deviation. Tables of room temperature values of refractive index are presented as a function of wavelength. Also given are the parameters for a three term Sellmeier equation for refractive index. Data are given for the following materials: commercially grown KCl; reactive atmosphere processed (RAP) KCl; KCl nominally doped with 1.5% KI; hot forged CaF_2; fusion cast CaF_2; CaF_2 doped with the following percentages of Er: 0.001%, 0.003%, 0.01%, 0.03%, 0.1%, 0.3%, 1% and 3%; chemical vapor deposited (CVD) ZnSe (2 specimens); and CVD ZnS (2 specimens).

The measurement of linear thermal expansion coefficient is discussed in Section 2.2. A table of linear thermal expansion coefficients as a function of temperature over the temperature -180 °C to 200 °C is given for the following materials: Al_2O_3, BaF_2, CaF_2, CdF_2, KBr, KCl, LiF, MgF_2, NaCl, NaF, SrF_2, ZnS (CVD), and ZnSe (CVD). The data are a synthesis of values from the literature and values obtained under this program. Our data are presented when disagreement with the literature was found. Graphs are shown to demonstrate the discrepancies.

The measurement of thermo-optic constants is discussed in Section 2.3. Tables of thermo-optic constants as a function of temperature over the temperature range -180 °C to 200 °C are presented. In the following table, the materials and wavelengths for which data are presented are denoted by x's:

Material/Wavelength	0.458 μm	0.6328 μm	1.15 μm	3.39 μm	10.6 μm
Al_2O_3	x	--	--	--	--
BaF_2	x	x	x	x	x
CaF_2	x	x	x	x	--
CdF_2	x	x	x	x	--
KBr (RAP)	x	x	x	x	x
KCl (RAP)	x	x	x	x	x
LiF	x	x	x	x	--
MgF_2	x	x	x	x	--
NaCl	x	x	x	x	--
NaF	x	x	x	x	--
SrF_2	x	x	x	x	x
ZnS (CVD)	--	--	x	x	x
ZnSe (CVD)	--	x	x	x	x

The measurement of piezo-optic constants and elastic compliances is discussed in Section 2.4. The piezo-optic constants of the following materials are given: As_2S_3 glass, BaF_2, CaF_2, Ge, KCl, fused SiO_2, SrF_2, a chalcogenide glass (Ge 33%, As 12%, Se 55%) and ZnSe (CVD).

1.4 Department of Defense Implications

The Department of Defense is currently constructing high-power laser systems. Criteria are needed for determining the suitability of different materials for use as windows in these systems. The measurements we perform provide data that laser system designers can use for determining the optical performance of candidate window materials.

1.5 Implications for Further Research

While extensive measurements of refractive properties have been made in the infrared, there remains a significant lack of data in the ultraviolet. A review of the literature indicates that piezo-optic data in the ultraviolet are virtually nonexistent and although some thermo-optic data are available, they are scant. These data would be particularly important for materials to be used in conjunction with excimer lasers (XeF, KrF, ArF).

4

2.   Technical Report

2.1   Introduction

With the development of new laser systems of ever increasing average-power levels, the optical elements in these systems, even if they possess extremely small absorption coefficients, can experience a significant temperature rise. The temperature distribution in the element will generally be nonuniform; hence, an optical beam propagating through the element will experience a wavefront distortion due to the thermally induced optic path variation across the aperture of the element. Theoretical analyses [1-4] have shown that the variation of optic path will depend on: (1) the change of refractive index with temperature, (2) the change of element thickness due to thermal expansion, (3) the change of refractive index due to stresses produced by thermal gradients and, (4) the change of thickness due to these stresses. In order to predict the magnitude of these effects, the optical designer requires certain material parameters which include absorption coefficient, refractive index n, thermo-optic constant dn/dT, piezo-optic constants q_{ij}, linear thermal expansion coefficient α, and elastic constants c_{ij} or s_{ij}. The purpose of the Optical Materials Characterization Program at the National Bureau of Standards has been to measure n, dn/dT, q_{ij}, α, and, when necessary s_{ij} of important optical materials of potential application in high-power laser systems. An earlier examination of the literature had shown that data on dn/dT and q_{ij} of important optical materials were almost nonexistent outside the visible region of the spectrum [5]; hence, our program has emphasized measurements in the infrared at 10.6 µm and 3.39 µm, wavelengths close to the output of CO_2 and DF lasers, respectively.

This report discusses the various techniques we use for measuring n, dn/dT, α, q_{ij}, and s_{ij}. It then summarizes, principally in tabular form, data we have obtained on a wide variety of infrared transmitting materials.

2.2   Refractive Index

Several techniques are used for measuring the refractive indices of optical materials; however, as part of this program, the measurements of n have been conducted on two precision spectrometers by the method of minimum deviation [6,7]. Schematic diagrams of both spectrometers are shown in Figure 1. The first spectrometer, which contains glass optics, is capable of measuring n in the visible and in the near infrared to an accuracy of several parts in 10^6. The second spectrometer, which contains mirror optics, is capable of measuring n from 200 nm in the ultraviolet to 50 µm in the infrared to an accuracy of several parts in 10^5. The accuracy depends on specimen quality and size. All values of refractive index are measured relative to the refractive index of air, n_a, that is we measure n/n_a. The value of n_a is about 1.0003 over the full wavelength range of measurement.

When determining the refractive index by the minimum deviation technique, collimated radiation is passed through a specimen which is in the form of a triangular prism. The prism is rotated about an axis parallel to the prism apex until a position is found where the angular deviation of the beam at a chosen wavelength is a minimum. In terms of the minimum deviation angle D, the angle between the emergent beam and an undeviated beam, and the prism angle A, the refractive index is given by

$$n = \frac{\sin \frac{D+A}{2}}{\sin \frac{A}{2}} \tag{1}$$

Measurements are performed at discrete wavelengths which are selected from the emission spectra of Hg, Cd, He, Cs, and Zn and from calibrated absorption bands of H_2O, polystyrene, methycyclohexane, and 1,2-4 trichlorobenzene. A series of calibrated narrow-band filters is also used in the infrared region. Each set of experimental data is fitted by a least squares solution to a three term Sellmeier-type dispersion equation of the form [8]

$$n^2 - 1 = \sum_{j=1}^{3} \frac{A_j \lambda^2}{\lambda^2 - \lambda_j^2} \tag{2}$$

5
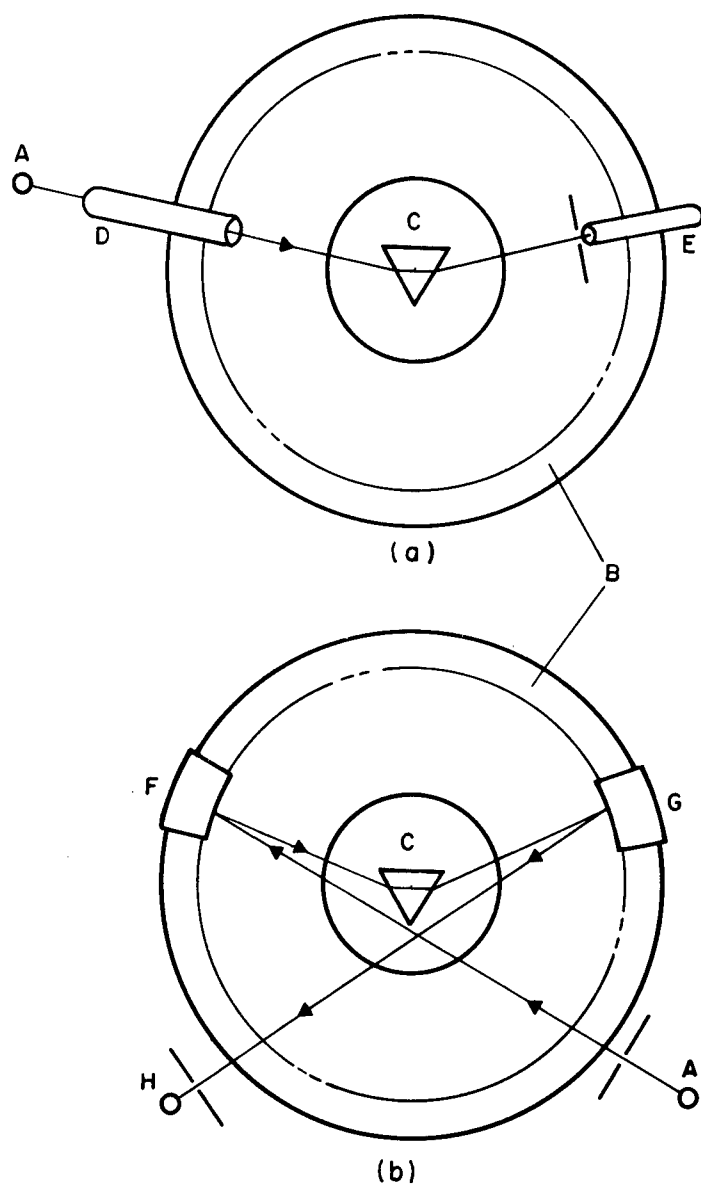
Figure 1. (a) Schematic of spectrometer used for visible region
refractometry. (b) Schematic of spectrometer used for non-
visible region refractometry. Symbols: A = source,
B = divided circle, C = prism table, D = collimator,
E = telescope, F = collimating mirror, G = movable mirror,
H = detector.

where λ is the wavelength of interest, λ_j is the wavelength position of an oscillator, and A_j is the oscillator strength. The λ_j's and A_j's are not intended to have any physical significance because they can be influenced by the wavelength range of the experiment data. Primary emphasis is given to procuring a mathematical fit to the measured data useful for interpolation. Equation (2) is not adequate for fitting data close to an absorption edge.

It is possible to obtain dn/dT by measuring n at two temperatures, usually near 20 °C and 30 °C (strictly speaking we obtain $\Delta n/\Delta T$). What we actually obtain is $d(n/n_a)/dT$ where

$$\frac{d}{dT} \left(\frac{n}{n_a}\right) \cong \frac{dn}{dT} - n \frac{dn_a}{dT} \qquad (3)$$

where $\frac{dn_a}{dT}$ is about $1.1 \times 10^{-6} K^{-1}$ [9]. The particular application of the data will determine whether the corrections in eq. (3) should be considered. For example, if the optical component is always in thermal equilibrium with the surrounding air, the correction is unnecessary.

In Tables 1a through 1e (Section 2.9) we tabulate coefficients for computing refractive index from equation (2) for the following materials: Table 1a - commercial KCl, RAP KCl, and KCl:KI (KCl nominally doped with 1.5% KI); Table 1b - hot forged and fusion cast CaF_2; Table 1c - SrF_2; Table 1d - CVD ZnS (2 specimens), and; Table 1e - CVD ZnSe (2 specimens).

In Tables 2a through 2f we present tabulations of refractive index at convenient wavelength intervals for the following materials: Table 2a, 2b, 2c-commercial KCl, RAP KCl, and KCl:KI; Table 2d, 2e- hot forged and fusion cast CaF_2; Table 2f - SrF_2; Table 2g, 2h - CVD ZnS (2 specimens); Table 2i, 2j - CVD ZnSe (2 specimens); and Table 2k - CaF_2 doped with the following percentage of Er: 0.001%, 0.003%, 0.01%, 0.03%, 0.1%, 0.3%, 1%, 3%. The values given apply to the specific specimens measured. Differences in the fourth decimal place may occur in nominally identical materials, as can be seen, for example, in the data for CVD ZnS and ZnSe.

2.3 Linear Thermal Expansion Coefficient

Different techniques have been used to measure linear thermal expansion. The most common technique employs a quartz dilatometer, but this measurement is not of great accuracy. A second technique involves the measurement as a function of temperature of lattice parameters by x-ray techniques [10]. In a third technique, α is obtained from a measurement of the capacitance of a parallel plate capacitor, where the plate spacing is a function of the specimen thickness [11]. We measure α by an interferometric technique [12]. A specially prepared specimen is placed between two optic flats as shown in Figure 2. Fizeau interference figures are observed when monochromatic radiation from a helium-neon laser ($\lambda = 0.6328$ µm) is reflected from the two surfaces in contact with the specimen. These fringes are observed to shift as a function of temperature due to the thermal expansion of the specimen.

Figure 3 shows a schematic diagram of the apparatus used for measuring both α and dn/dT. This apparatus will operate over the temperature range -180 °C to 200 °C. The furnace is constructed from a cylinder of copper 37 mm in diameter by 75 mm high with walls 6 mm thick to permit rapid transfer of heat. A commercial band heater, which is clamped around the furnace generates 175 W of heat with an input of 120 VAC.

The furnace rests at the bottom of an evacuable chamber 100 mm in diameter by 150 mm tall. Protruding from the bottom is a copper rod, 12 mm in diameter by 150 mm long, that conducts heat away from the furnace to the liquid nitrogen reservoir. Thus, we can stabilize the temperature in the furnace by balancing the heat input from the heater with the heat leak to the liquid nitrogen.
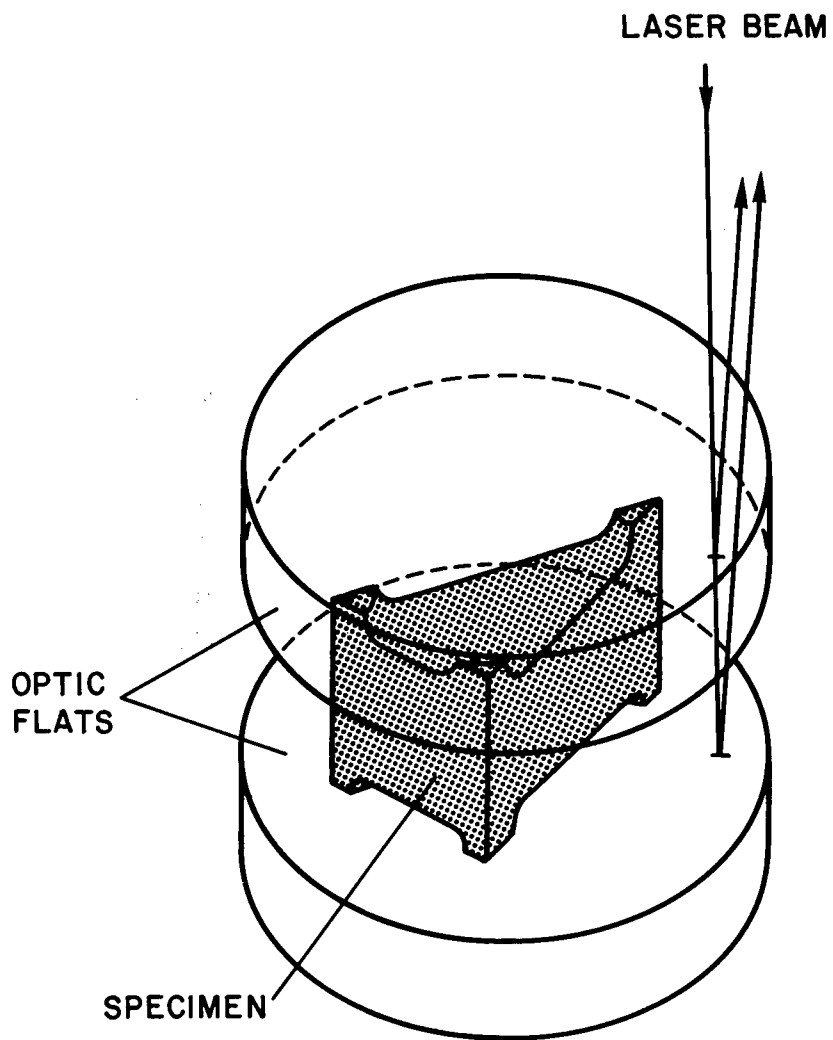
LASER BEAM

OPTIC
FLATS

SPECIMEN

Figure 2. Fizeau interferometer for measuring linear thermal expansion.

LASER BEAM

MIRROR

ELECTRICAL
FEED THROUGHS

WINDOW

LOW PRESSURE
HELIUM

WINDOW
COPPER FURNACE

SPECIMEN
HEATER
THERMOCOUPLES

COPPER ROD

CRYOSTAT

LIQUID N$_2$
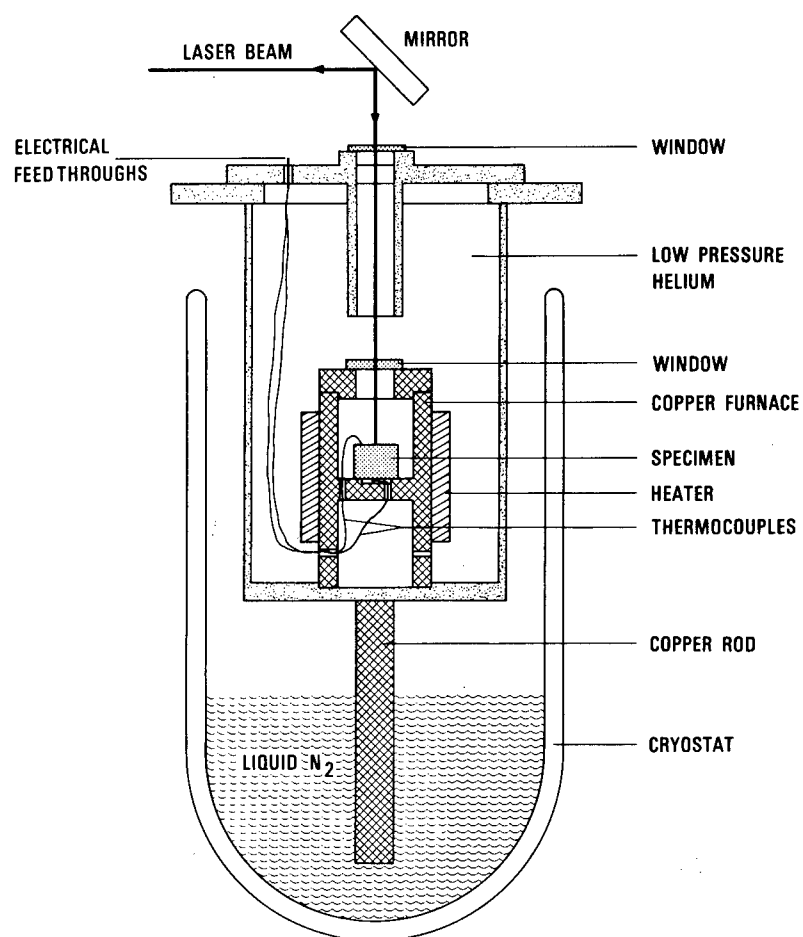
Figure 3. Apparatus for measuring linear thermal expansion and thermo-
optic constants as a function of temperature over the range
-180 °C to 200 °C.

9

The specimen rests within the furnace over a depression that is milled at an angle of 1° with respect to the furnace axis in order to deflect extraneous laser beam reflections to the side. Holes are drilled at several locations within the furnace to allow placement of thermocouples in contact with the specimen and to allow the pressure within the furnace to equalize with the pressure outside the furnace. Two thermocouples measure the temperature at the top and at the bottom of the specimen. A copper cover with a window allows access of laser radiation to the specimen in the furnace while maintaining a uniform thermal environment around the specimen. All windows in the system are tilted at a 1° angle to eliminate unwanted reflections.

We find that the system operates well when filled with a helium exchange gas of several millimeters Hg pressure. The helium environment has several advantages over air or vacuum. During cool-down, products in the air condense on the system optics and hence interfere with the laser beam. With vacuum, the thermal response of the system is sluggish because of poor heat transfer between the furnace, the heat leak, and the specimen. In addition, there is a large temperature difference between the two thermocouples. With the helium present, the maximum temperature differential measured with the two thermocouples across a 12 mm thick specimen is less than 1 K at a given mean temperature.

The procedure used for measuring α consists of first cooling the specimen to approximately liquid nitrogen temperature. Sufficient time is allowed for the two thermocouple readings to agree to within 1 K. The furnace is then heated very slowly until a fringe minimum is observed on a strip chart recorder monitoring the Fizeau intensity. The temperature is then recorded. Subsequently, the furnace is heated rapidly and after a convenient number of fringes has been observed, power to the furnace is cut back to allow the thermocouple readings to equilibrate while the temperature is slowly rising. At a fringe minimum, the temperature is recorded. The heating process is repeated until the maximum desired temperature is achieved.

The linear thermal expansion coefficient is defined by

$$\alpha = \frac{1}{t_o} \frac{dt}{dT} \tag{4}$$

where t_o is the room temperature specimen thickness and t is the specimen thickness at temperature T. In terms of a fringe count N_i at a temperature T_i we calculate $\alpha(T)$ by the formula

$$\alpha(T) = \frac{\lambda}{2t_o} \frac{N_i - N_{i-1}}{T_i - T_{i-1}} \tag{5}$$

where $T = (T_i + T_{i-1})/2$. A graph is then made of α as a function of T. On this graph we also plot either the accepted handbook values of $\alpha(T)$ when they are available, or else values from the literature. A curve is then visually drawn through the data and from this curve, we abstract a set of data points. These points are then fitted by computer to a polynominal. The purpose of the fit is to obtain an analytical expression for $\alpha(T)$, which is needed for computing dn/dT as a function of temperature.

In Table 3, we present values of α from -180 °C to 200 °C at 20 ° temperature intervals for Al_2O_3 (only perpendicular to c-axis, $\alpha_\perp$), BaF_2, CaF_2, CdF_2, KBr, KCl, LiF, MgF_2 (both $\alpha_{||}$ and $\alpha_\perp$), NaCl, NaF, SrF_2, CVD ZnS, and CVD ZnSe. In the cases of NaCl and NaF there is disagreement between published values [13] and our values (see figures 4 and 5); we list only our values. We have confidence in our values because our results are in excellent agreement with the bulk of the measurements reported in the literature. We did not measure the linear thermal expansion coefficient of Al_2O_3; hence, the numbers shown were computed from values in the American Institute of Physics Handbook [13].

Figures 4 and 5 show the discrepancies betweeen our values (triangles and dashed lines) and values in the literature (circles and solid lines) for NaCl and NaF, respectively. In Figures 6 and 7, we show curves of α as a function of temperature for CdF_2 and MgF_2, respectively. The triangles and solid curves are our data. In the case of CdF_2, there has been virtually no earlier published data. In the case of MgF_2, we find excellent agreement with recently obtained low temperature data [11] but agreement with others [10,14] is poor above room temperature.

10
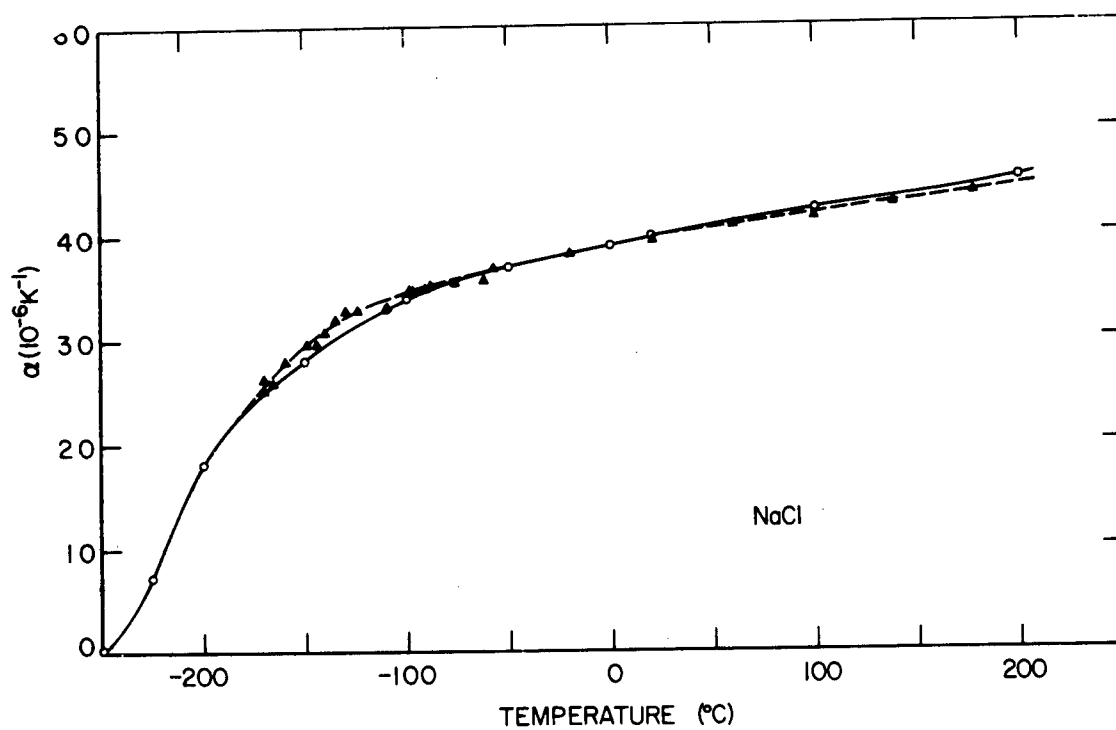
Figure 4. Linear thermal expansion coefficient of NaCl as a function
of temperature. The triangles are our experimental data and
the circles are from the AIP Handbook [13].
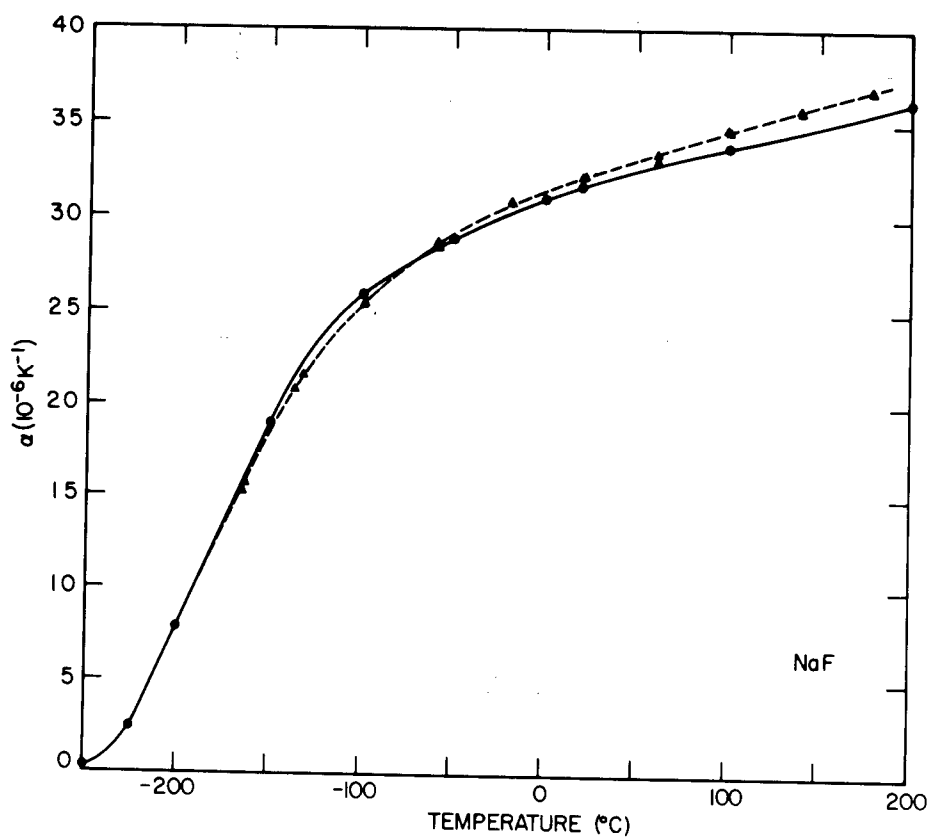
Figure 5. Linear thermal expansion coefficient of NaF. The triangles
are our experimental data and the circles are from the AIP
Handbook [13].
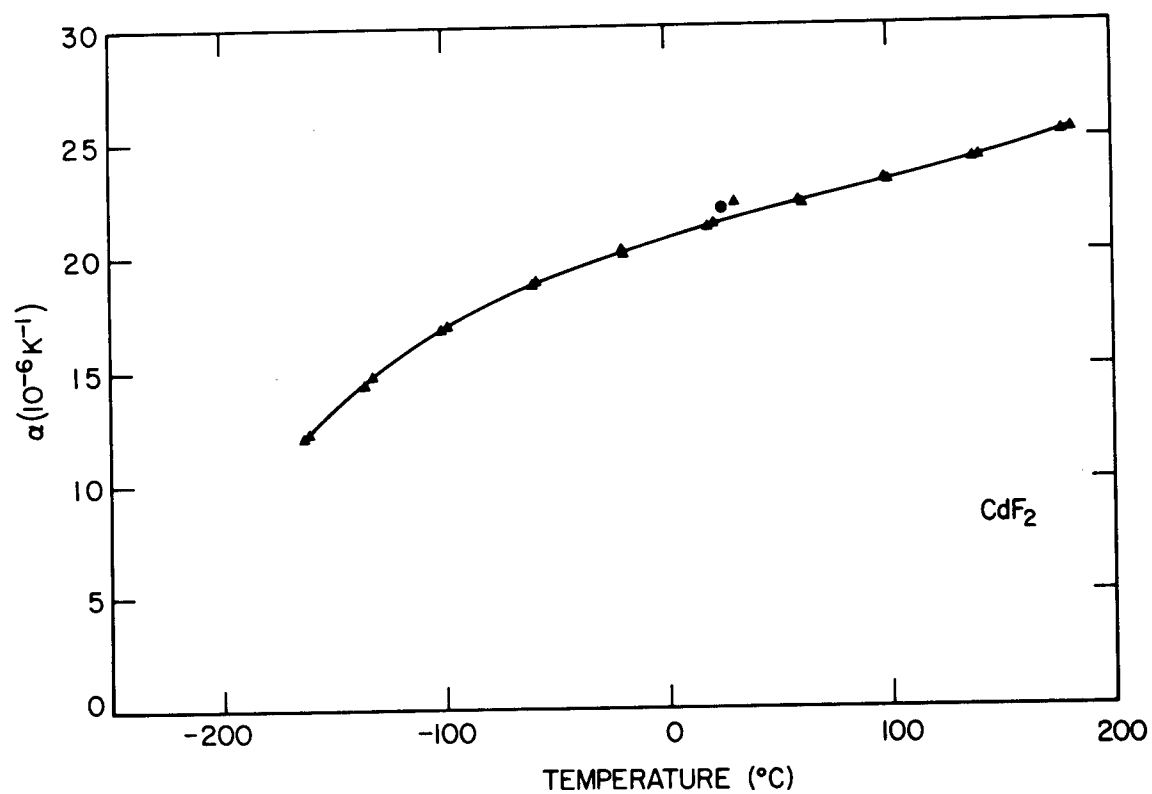
Figure 6. Linear thermal expansion coefficient of CdF_2 as a function of temperature. The triangles show our experimental data and the single circle is from S. S. Ballard and J. S. Browder, Appl. Opt. 5, 1873 (1966).
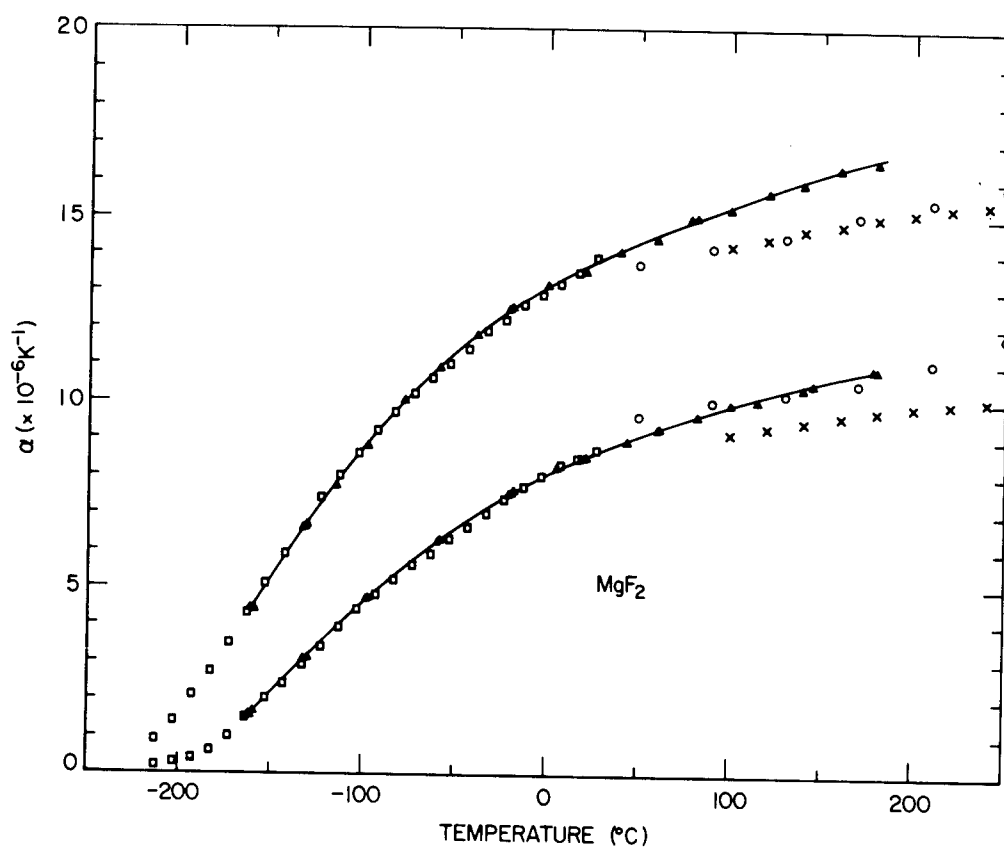
Figure 7. Linear thermal expansion coefficients of single crystal MgF_2 as a function of temperature. The upper curve is for $\alpha_{||}$; the lower curve is for $\alpha_\perp$. $||$ and $\perp$ refer to parallel and perpendicular to the c axis, respectively. The curves and triangles are our data; the squares are from Ref. [11], the circles from Ref. [10], and the x's from [14].

14

2.4 The Thermo-optic Constant

The thermo-optic constant, dn/dT, is measured by an interferometric technique at discrete laser wavelengths over the temperature range -180 °C to 200 °C. With this technique, we observe as a function of temperature the shift of Fizeau interference fringes formed from reflections off the surfaces of an optical specimen polished plane parallel. The same apparatus and experimental technique used for measuring α is used for measuring dn/dT. The change of index from room temperature to temperature T_i is given by

$$\Delta n(T_i) = \left(\frac{M_i \lambda}{2t_o} - n_o \frac{\Delta t}{t_o} \right) (1 + \frac{\Delta t}{t_o})^{-1} \qquad (6)$$

where M_i is the fringe count from room temperature to temperature T_i, n_o is the room temperature refractive index, and $\Delta t/t_o$ is computed at temperature T_i from the linear thermal expansion data. We obtain dn/dT (strictly speaking $\Delta n/\Delta T$) from

$$\frac{dn(T)}{dT} = \frac{\Delta n(T_i) - \Delta n(T_{i-1})}{T_i - T_{i-1}} \qquad (7)$$

where $T = (T_i + T_{i-1})/2$.

Table 4 presents thermo-optic constants of the following materials over the temperature range -180 °C to 200 °C tabulated at 20 °C increments:

Al_2O_3 – Table 4a MgF_2 – Table 4h

BaF_2 – Table 4b   NaCl – Table 4i

CaF_2 – Table 4c   NaF – Table 4j

CdF_2 – Table 4d SrF_2 – Table 4k

KBr – Table 4e   ZnS(CVD) – Table 4l

KCl – Table 4f   ZnSe(CVD) – Table 4m

LiF – Table 4g

An intercomparison of some of these data with data in the literature has been made and reasonably good agreement was found [15].

In Table 5 we present refractive index and thickness data used for calculating dn/dT of the above-mentioned materials.

2.5 Piezo-optic Constants

The piezo-optic constants are the components of a fourth rank tensor that describe the effect of stress on the refractive index of a material [16]. The relationship is expressed by

$$\Delta(\kappa^{-1})_{ij} = q_{ijkl} \, \sigma_{kl} \qquad (8)$$

where κ^{-1} is the reciprocal of the optical dielectric tensor, σ is the stress tensor, q_{ijkl} are the components of the piezo-optic tensor, and the indices, i, j, k, and l take values 1, 2, and 3. Repeated indices indicate summation. Because both the stress and dielectric tensors are symmetric under interchange of indices, a contracted notation (also called the Voigt notation) has been adopted so that equation (8) becomes

$$\Delta(\kappa^{-1})_m = q_{mn} \, \sigma_n \qquad (9)$$

where m and n take on values 1-6 corresponding to ij $\rightarrow$ m, kl $\rightarrow$ n with 11 $\rightarrow$ 1, 22 $\rightarrow$ 2, 33 $\rightarrow$ 3, 23 and 32 $\rightarrow$ 4, 13 and 31 $\rightarrow$ 5, and 12 and 21 $\rightarrow$ 6. Nye [16] discusses in detail the relationship between components in the full notation and in the contracted notation.

15

The elasto-optic constants relate the change of refractive index to strain in a material. These coefficients are related to the piezo-optic constants by

$$p_{ij} = q_{im}c_{mj} \qquad (10)$$

where p_{ij} is a component of the elasto-optic tensor and c_{ij} is a component of the elastic stiffness tensor, both expressed in contracted notation. In this presentation, only the measurement of piezo-optic constants is discussed; however, by use of equation (10), it is a simple matter to convert to the elasto-optic constants.

In a crystalline material with the least symmetry there exist 36 independent piezo-optic coefficients. However, the materials that have been of interest to the NBS program have been of cubic or isotropic symmetry; hence, the discussion is limited to these materials. Most cubic materials possess three independent piezo-optic constants, q_{11}, q_{12}, q_{44}; isotropic materials have two independent constants, q_{11} and q_{12}, where $q_{44} = q_{11} - q_{12}$. Thus, we can measure all these coefficients by measuring changes of n when stresses are applied along certain symmetry directions. If we apply a uniaxial compressive stress, P, along the [100] axis of a cubic material (any axis of an isotropic material), the change of n will depend on the state of polarization of the radiation and is given by

$$\Delta n = \frac{n^3}{2} q P \qquad (11)$$

where $q = q_{11}$ for radiation polarized parallel to the stress axis and $q = q_{12}$ for radiation polarized perpendicular to the stress axis. This convention will be used throughout the following discussion.

The stress-induced birefringence (piezo-birefringence) for P along [100] is given by

$$\Delta n_{||} - \Delta n_{\perp} = \frac{n^3}{2} (q_{11} - q_{12}) P \qquad (12)$$

and for P along [111] is given by

$$\Delta n_{||} - \Delta n_{\perp} = \frac{n^3}{2} q_{44} P. \qquad (13)$$

Here $||$ and $\perp$ refer, respectively, to polarization parallel and perpendicular to the stress axis. Equations [11-13] provide more than enough conditions for obtaining all the piezo-optic coefficients.

A variety of techniques have been employed for measuring the photoelastic constants of optical materials including acousto-optic scattering and Brillouin scattering. Many of these techniques have been reviewed recently [17]. In this article, we discuss the techniques used in the NBS measurements program. The techniques involve interferometric and polarimetric measurements on specimens under static uniaxial and hydrostatic stress. These measurements can provide data for obtaining not only the piezo-optic constants, but also elastic compliances.

Fizeau Interferometer: A specimen in the form of a right rectangular prism with dimensions approximately 12 x 12 x 36 mm is stressed parallel to the long dimension in a calibrated stressing frame [18] (see Figure 8). Two opposite rectangular faces of the prism are polished flat and parallel so that Fizeau interference fringes are observed when laser radiation is reflected from them. These fringes are observed to shift as a function of applied stress. If the stress is applied along the [100] crystallographic axis, the fringe shift per unit applied stress is

$$\frac{\Delta N}{\Delta P} = \frac{2t}{\lambda} (\frac{n^3}{2} q - n s_{12}). \qquad (14)$$

where s_{12} is a component of the elastic compliance tensor and q is defined above. If the specimen is subjected to a hydrostatic compression, the fringe shift per unit applied pressure is

$$\frac{\Delta N}{\Delta P} = \frac{2t}{\lambda} \left[\frac{n^3}{2} (q_{11} + 2q_{12}) - n(s_{11} + 2s_{12}) \right]. \qquad (15)$$

16
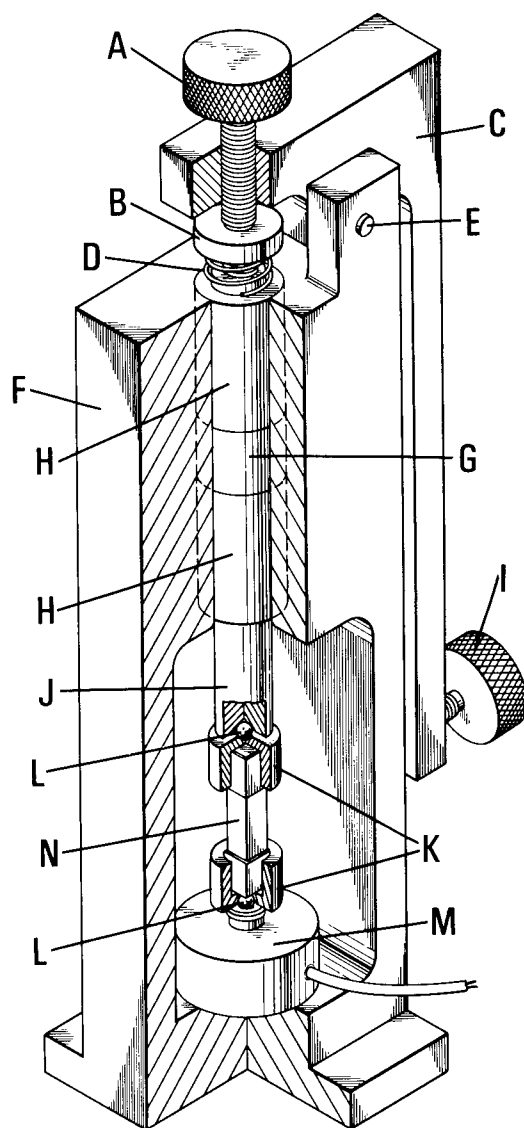
Figure 8. Stressing apparatus. A = adjustment screw with domed tip, B = adjusting member threaded into push rod, C = lever arm, D = coil spring, E = axis, F = frame, G = spacer, H = ball bushing, I - stressing screw with domed tip, J = push rod, K = specimen cup, L = steel ball, M = load cell, N = specimen.

The extra terms containing the elastic compliances on the right of equations (14) and (15) occur because the fringe shift is due to the change of optic path in the specimen, which depends both on the change of n and the change of specimen thickness.

Twyman-Green Interferometer: A specimen mounted in a calibrated stressing frame is placed in one arm of a Twyman-Green interferometer. When a stress is applied to the specimen the fringes at the output of interferometer are observed to shift. If the stress is applied along the [100] crystallographic axis, the fringe shift per unit applied stress is

$$\frac{\Delta N}{\Delta P} = \frac{2t}{\lambda} \left[\frac{n^3}{2} q - (n-1)s_{12} \right] \qquad (16)$$

If all the measurements described by equations [14-16] are made, we can obtain not only q_{11} and q_{12}, but also s_{11} and s_{12}.

Modified Twyman-Green Interferometer. For many cases, especially in the infrared, it is difficult to obtain a shift of even one fringe by the above two methods. We then require a modified interferometric technique which is capable of measuring fractions of a fringe shift [19,20]. Figure 9 shows an interferometer that is capable of measuring 0.01 fringe shift at 10.6 µm. The two arms of the interferometer are in close proximity in order to minimize instabilities due to air currents and vibrations. The effects of vibrations are also minimized by mounting the diagonal mirror onto the same base as the beamsplitter and by mounting the two end mirrors on a common base. The end mirror in the specimen arm of the interferometer undergoes a sinusoidal translation along the optic axis, thus, modulating the output intensity of the interferometer. The reference specimen at 10.6 µm is a crystal of Ge in a compression appratus that we have calibrated by measuring the force necessary to produce an integral number fringe shift. Fractional fringes are then obtained by linear interpolation. In operation, the reference specimen is stressed until the interferometer is at a null, which occurs when the fundamental harmonic of the output intensity is zero. A given stress applied to the unknown specimen will shift the interferometer away from null, whereupon we compensate for this shift by applying an incremental stress to the Ge that brings the interferometer back to null. From these data we can calculate q_{11} and q_{12} with eq. (16) provided s_{12} is known. The state of the polarization is determined by the polarizer. The variable wave plate is used to balance the intensities of the two arms of the interferometer for a given state of polarization. It consists of a specimen of Ge placed in a stressing apparatus with the angle of stress at 45° with respect to the vertical in a plane perpendicular to the beam axis.

Modified Dyson Interferometer. We have constructed a polarizing interferometer for measuring photoelastic constants. This instrument is capable of measuring fringe shifts to a precision of $\lambda/500$ at 632.8 nm [21]. It is based on a design by Dyson [22] that was further modified by Green [23]. A schematic diagram of the experimental apparatus is shown in Figure 10. This instrument operates on two beam interference, however, the two beams are orthogonally polarized. Thus, an optic path change in one arm of the interferometer results in a change of state of polarization of the combined beam at the output of the interferometer. Hence, fringe shifts are analyzed with ellipsometric techniques which have great inherent precision.

This interferometer has several other advantages over conventional Twyman-Green interferometers: it is more stable with respect to motion of system elements because both beams traverse the same optics, hence, the optic path changes in both arms tend to be equal. In addition, the close proximity of the arms minimizes the effects of thermal currents, which are further reduced by placement of a cover over the interferometer part of the apparatus.

In this interferometer, the expression for the piezo-optic constant in terms of the fringe shift per unit applied stress is

$$q = \frac{2}{n^3} \left[\frac{\lambda}{t} \frac{\Delta N}{\Delta P} + (n-1)s_{12} \right] \qquad (17)$$

Stress-Induced Birefringence (Piezo-Birefringence): The coefficients that determine stress-induced birefringence in most cubic materials are $q_{11}-q_{12}$ and q_{44}. It is most convenient to measure these coefficients on two separate samples, one oriented for stress along [100] and the other oriented for stress along [111], because in these orientations the crystal becomes optically uniaxial and not biaxial; hence, small angular misorientations lead to only small measurement errors.

18
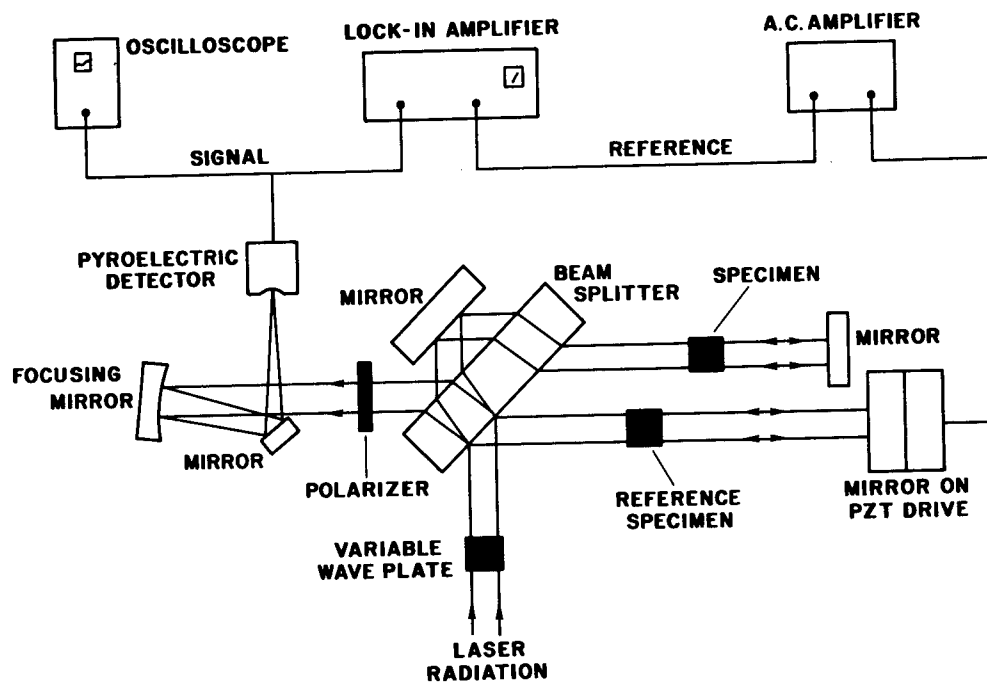
Figure 9. Modified Twyman-Green interferometer for measuring piezo-optic constants at 10.6 μm.

SILICON MATRIX VIDICON

ANALYSER

SOLEIL-BABINET COMPENSATOR

SPATIAL FILTER AND
BEAM EXPANDER

MIRROR

LENS

POLARIZER

WOLLASTON PRISM

LENS

E   O

E

O

LASER

SPECIMEN

LENS

QUARTER WAVE PLATE

MIRROR
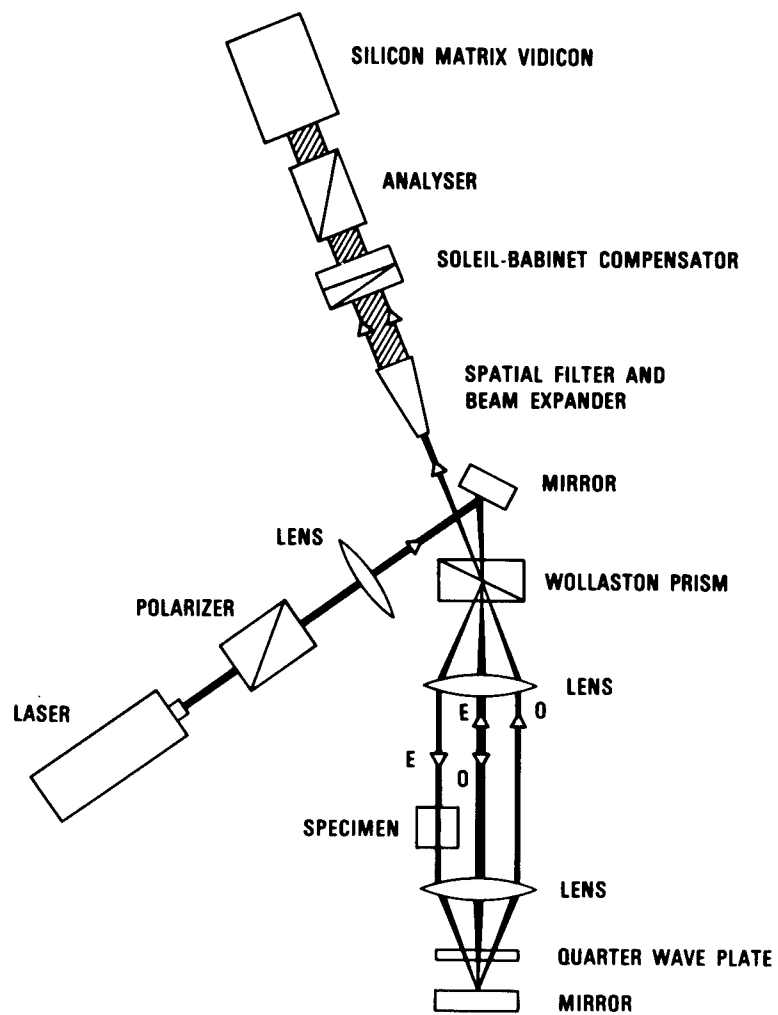
Figure 10. Modified Dyson interferometer for measuring piezo-optic
           constants in the visible.

20

A variety of techniques have been used to measure piezo-birefringence [17]. In the simplest technique, the specimen is placed between two crossed polarizers with the stress axis at 45° with respect to the direction of polarization and perpendicular to the radiation beam. As stress is applied, the output intensity will undergo a series of nulls corresponding to a series of fringe shifts and the fringe shift per unit applied stress is

$$\frac{\Delta N}{\Delta P} = \frac{tn^3}{2\lambda} q'$$ (18)

where $q' = q_{11}-q_{12}$ for stress along [100] and $q' = q_{44}$ for stress along [111]. In the case of noncubic materials, the expression for the fringe shift becomes much more complicated.

Frequently, it is either impossible or inconvenient to apply sufficient stress to obtain the shift of even one fringe. In this case, a compensator is placed within the experimental apparatus. Compensators used are Soleil compensators, de Senarmont compensators, or compensators consisting of a stressed specimen which acts like a Soleil compensator. Photometric techniques are also employed [24]. Recently, Birnbaum et al. [25] have developed an interesting new technique for measuring piezo-birefringence in which a stressed specimen is placed in a scanning Fabry-Perot cavity.

A simple variation of the basic crossed polarizer technique, is to double pass the radiation through the specimen [20]. This technique which has the advantage of requiring only one polarizer, has double the sensitivity of the single pass method. Figure 11 shows a double pass arrangement for measuring piezo-birefringence at 10.6 μm.

In Tables 6 through 11, we present photoelastic constant data for CaF_2, SrF_2, BaF_2, As_2S_3 glass, a chalcogenide glass (Ge 33%, As 12%, Se 55%), Ge, KCl, KCl:KI, fused SiO_2, and CVD ZnSe. The ZnSe is a polycrystalline material and, hence, is considered to be isotropic. In Table 12, we present elastic constant data for BaF_2, CaF_2, Ge, KCl, fused SiO_2, SrF_2, and ZnSe (CVD).

2.6 Publications

A. Feldman, D. Horowitz and R. M. Waxler, "Stress Optic Measurements in the Infrared", in the Proceedings of the Third Conference on High Power Infrared Laser Window Materials, Nov. 12-14, 1973, Edited by C. A. Pitha and B. Bendow, AFCRL-TR-74-0085 (1), Special Reports, No. 174, p. 403, February, 1974.

A. Feldman, I. Malitson, D. Horowitz, R. M. Waxler and M. J. Dodge, "Characterization of Infrared Laser Window Materials at the National Bureau of Standards", in Laser Induced Damage in Optical Materials: 1974, NBS Special Publication 414, eds. A. J. Glass and A. H. Guenther (U.S. GPO SD Catalogue No. C13.10:414, 1974), pp. 141.

A. Feldman, I. H. Malitson, D. Horowitz, R. M. Waxler, and M. J. Dodge, "Optical Properties of Polycrystalline ZnSe", in proceedings of the Fourth Annual Conference on Infrared Laser Window Materials, Tucson, AZ (Nov. 1974), pp. 117.

A. Feldman, D. Horowitz and R. M. Waxler, "Photoelastic Constants of Infrared Materials", in Laser Induced Damage in Optical Materials: 1975, NBS Special Publication 435, Eds. A. J. Glass and A. H. Guenther, (US GPO, 1976), pp. 164.

M. J. Dodge and I. H. Malitson, "Refractive Index and Temperature Coefficient of Index of CVD Zinc Selenide, in Laser Induced Damage in Optical Materials: 1975, NBS Special Publication 435, Eds. A. J. Glass and A. H. Guenther, (US GPO, 1976) pp. 170.

A. Feldman and W. J. McKean, "Improved Stressing Apparatus for Photo-elasticity Measurements", Rev. Sci. Instrum. 46, 1588 (1975).

A. Feldman, R. M. Waxler and D. Horowitz, "Measuring Photoelastic and Elastic Constants of Transparent Materials by Application of Static Stress", in Optical Properties of Highly Transparent Solids, Edited by S. S. Mitra and B. Bendow (Plenum Publishing Corporation, New York, 1975), pp. 517.

FOCUSING MIRROR

MIRROR

PYROELECTRIC
DETECTOR

VARIABLE
WAVE PLATE

LASER
RADIATION

BEAM STOP

BEAM SPLITTER

CHOPPER

POLARIZER

COMPENSATOR

SPECIMEN

MIRROR
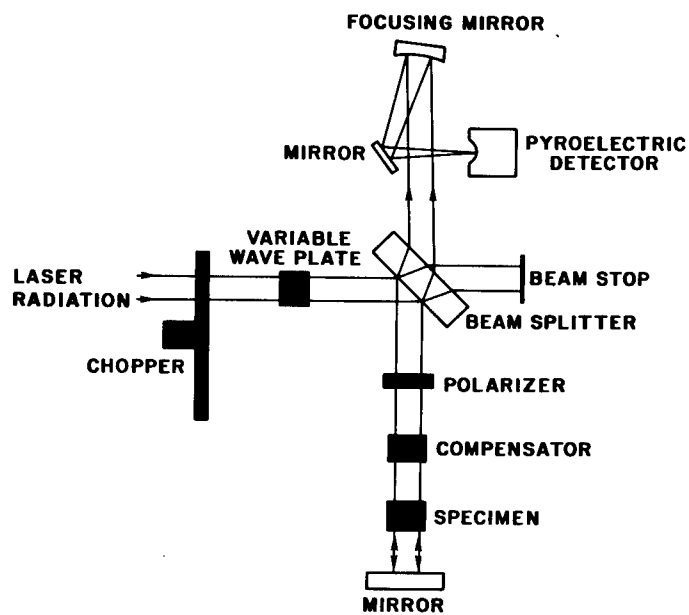
Figure 11. Double pass arrangement for measuring piezo-birefringence
at 10.6 µm.

A. Feldman, D. Horowitz and R. M. Waxler, "Piezo-Optic Constants in the Infrared", in Procee-dings of the Fifth Annual Conference on Infrared Laser Window Materials, Las Vegas, Nev., December 1975.

M. J. Dodge, "Refractive Index of High Purity KCl and KI Doped KCl", in Proceedings of the Fifth Annual Conference on Infrared Laser Materials, Las Vegas, NV, Dec. 1975 (1976). pp. 215.

A. Feldman, "Measuring the Optical Properties of Infrared Laser Windows", Electro-Optical Systems Design 8, 36 (1976). ·

A. Feldman, "Optical Properties of Infrared Laser Windows", in Proceedings of the Technical Program Electro-Optical Systems Design Conference-1976, International Laser Exposition, New York, New York, Sept. 14-16, 1976 (Industrial and Scientific Conference Management, Chicago 1976), pp. 499.

A. Feldman, D. Horowitz, and R. M. Waxler, "Effect of Temperature and Stress on the Refractive Index of Window Materials", in Laser Induced Damage in Optical Materials: 1976, NBS Special Publication 462, Eds. A. J. Glass and A. H. Guenther (US GPO SD Cat. No. 13.10:462, 1976), pp. 58.

M. J. Dodge, "Refractive Index and Temperature Coefficient of Refractive Index of Hot-Forged Calcium Fluoride", in Laser Induced Damage in Optical Materials: 1976, NBS Special Publication 462, eds. A. J. Glass and A. H. Guenther (US GPO SD Cat. No. 13.10:462, 1976) pp. 64.

R. M. Waxler, D. Horowitz and A. Feldman, "Precision Interferometer for Measuring Photoelastic Constants", Appl. Opt. 16, 20 (1977).

A. Feldman, D. Horowitz, and R. M. Waxler, "Refractive Properties of Infrared Window Materials", in Laser Induced Damage in Optical Materials: 1977, NBS Special Publication 509, Edited by A. J. Glass and A. H. Guenther (US GPO, 1978), pp. 74.

A. Feldman, D. Horowitz and R. M. Waxler, "Photoelastic Constants of Potassium Chloride at 10.6 μm", Appl. Opt. 16, 2925 (1977).

M. J. Dodge, "Refractive Properties of CVD Zinc Sulfide", in Laser Induced Damage in Optical Materials: 1977, NBS Special Publication 509, eds. A. J. Glass and A. H. Guenther (US GPO, 1978), pp. 83.

C. K. Kim, A. Feldman, D. Horowitz, and R. M. Waxler, "Temperature Dependence of Szigeti Effective Change of Alkali Halides", Solid State Communications, 25, 397 (1978).

A. Feldman, R. M. Waxler and D. Horowitz, "Photoelastic Constants of Germanium", J. Appl. Phys. 49, 2589 (1978).

A. Feldman, "Measurement of the Photoelastic Constants of Optical Materials", Optical Eng. 17, 453 (1978).

M. J. Dodge, "Refractive Index of SrF$_2$", in Laser Induced Damage in Optical Materials: 1978, to be published.

R. M. Waxler, A. Feldman and D. Horowitz, "Piezo-Optic Coefficients of Some Neodymium Doped Laser Glasses and Single Crystals of CaF$_2$, BaF$_2$ and SrF$_2$", in Laser Induced Damage in Optical Materials:1978, to be published.

A. Feldman and M. J. Dodge, D. Horowitz and R. M. Waxler, "The National Bureau of Standards Optical Measurements Program: Refractive Index, Thermo-Optic Constants and Photoelastic Constants", to be published.

2.7 Acknowledgements

2.8 References

1. M. Sparks, J. Appl. Phys. 42 5029 (1971).

2. J. R. Jasperse and P. D. Gianino, J. Appl. Phys. 43, 1686 (1972).

3. B. Bendow, P. D. Gianino, A. Hordvik and L. H. Skolnik, Optics Comm. 7, 219 (1973).

4. B. Bendow and P. D. Gianino, Appl. Phys. 2, 1 (1973).

5. C. S. Sahagian and C. A. Pitha, Compendium on High Power Infrared Laser Window Materials (LQ Program), AFCRL-72-0170, 9 March 1972, Special Reports No. 135.

6. L. W. Tilton, J. Res. Natl. Bur. Std., (U.S.), 2, 909 (1929), RP 64.

7. C. Weir, S. Spinner, I. H. Malitson and W. J. Rodney, J. Res. Natl. Bur. Std., (U.S.), 58, 189 (April 1957), RP 2751.

8. L. E. Sutton and O. N. Stavroudis, J. Opt. Soc. Am. 51, 901 (1961).

9. American Institute of Physics Handbook, (McGraw-Hill, 1972), p. 6-111.

10. K. V. Krishna Rao, S. V. Nagender Naidu and P. L. N. Setty, Acta Cryst. 15, 528 (1962).

11. J. S. Browder and S. S. Ballard, Appl. Opt. 16, 3214 (1977).

12. J. B. Saunders, J. Res. Natl. Bur. Std. (U.S.), 35, 157 (1945) RP 1668.

13. American Institute of Physics Handbook, Dwight E. Gray, ed. (McGraw-Hill Book Company, 1972) pp. 4-119.

14. Yep. Artyukh and V. N. Reytorov, Sov. J. Opt. Tech. 40, 523 (1973).

15. A. Feldman, D. Horowitz and R. M. Waxler, "Refractive Properties of Infrared Window Materials", in Laser Induced Damage in Optical Materials:1977, NBS Special Publication 509, Edited by A. J. Glass and A. H. Guenther, (US GPO 1977), pp. 74.

16. J. F. Nye, Physical Properties of Crystals (Oxford University Press, London 1957), pp. 243-254.

17. A. Feldman, Optical Eng. 17, 453 (1978).

18. A. Feldman and W. J. McKean, Rev. Sci. Instrum. 46, 1588 (1975).

19. A. Feldman, R. M. Waxler and D. Horowitz, "Measuring Photoelastic and Elastic Constants of Transparent Materials by Application of Static Stress" in Optical Properties of Highly Transparent Solids, Edited by S. S. Mitra and B. Bendow (Plenum Publishing Corporation, New York, 1975) pp. 517.

24

20. A. Feldman, D. Horowitz and R. M. Waxler, Appl. Opt. 16, 2925 (1977).

21. R. M. Waxler, D. Horowitz and A. Feldman, Appl. Opt. 16, 20 (1977).

22. J. Dyson, Interferometry as a Measuring Tool, (The Machinery Publishing Co., Ltd., Brighton, 1970).

23. F. Green, in Optical Instruments and Techniques, 1969, edited by J. H. Dickson (Oriel Press Limited, NewCastle upon Tyne, England, 1970), pp. 189-198.

24. A. J. Michael, J. Opt. Soc. Am. 58, 889 (1968).

25. G. Birnbaum, E. Cory and K. Gow, Appl. Opt. 13, 1660 (1974).

2.9 Tables

Table 1a. Constants of Dispersion Equation for KCl near 20 °C.

Specimen Temperature	Commercial 19.9 °C	RAP[a] 20.2 °C	KCl:KI[b] 19.9 °C
A_1	0.74783561	0.80902239	0.78085271
A_2	0.42626630	0.36511458	0.39493953
A_3	4.6867104	2.2323342	2.2662238
λ_1 (μm)	0.083633417	0.08828162	0.08611153
λ_2 (μm)	0.15389978	0.15737774	0.15600595
λ_3 (μm)	95.063422	65.870423	66.360157
No. of Wavelengths	79	58	54
Wavelength Range (μm)	0.22–14.4	0.25–15.5	0.25–15.5
Average Absolute Residual of n (10^{-5})	2.3	2.9	3.2

[a]Reactive atmosphere processed. [b]KCl nominally doped with 1.5% KI.

Table 1b. Constants of Dispersion Equation for CaF_2 near 20 °C.

Specimen Temperature	Hot Forged 20.8 °C	Fusion Cast 21.7 °C
A_1	0.98594551	0.34393190
A_2	0.05290246	0.6948269
A_3	4.2816899	3.8902192
λ_1 (μm)	0.07218116	0.0127821
λ_2 (μm)	0.14114719	0.0936663
λ_3 (μm)	36.465937	34.8259
No. of Wavelengths	69	60
Wavelength Range	0.25–8.03	0.21–8.7
Average Absolute Residual of n (10^{-5})	1.9	2.1

Table 1c. Constants of Dispersion Equation for Fusion Cast SrF_2 near 20 °C.

Specimen	Fusion Cast
Temperature	20 °C
A_1	0.67805894
A_2	0.37140533
A_3	3.3485284
λ_1 (μm)	0.05628989
λ_2 (μm)	0.10801027
λ_3 (μm)	39.906666
No. of Wavelengths	53
Wavelength Range (μm)	0.21-11.5
Average Absolute Residual of n (10^{-5})	2.1

Table 1d. Constants of Dispersion Equation for Chemical Vapor Deposited (CVD) ZnS near 20 °C.

Specimen	#1	#2
Temperature	21.6 °C	21.9 °C
A_1	0.33904026	0.24199447
A_2	3.7606868	3.8575584
A_3	2.7312353	2.5433609
λ_1 (μm)	0.31423026	0.33005445
λ_2 (μm)	0.17594174	0.17899635
λ_3 (μm)	33.886560	32.849275
No. of Wavelengths	25	30
Wavelength Range (μm)	0.55-10.6	0.55-10.6
Average Absolute Residual of n (10^{-5})	5.4	4.6

Table 1e. Constants of Dispersion Equation for Chemical Vapor
          Deposited (CVD) ZnSe near 20 °C.

Specimen	#1	#2
Temperature	20.3 °C	20.8 °C
A_1	4.2980149	4.4639521
A_2	0.62776557	0.46132463
A_3	2.8955633	2.8828867
λ_1 (µm)	0.19206300	0.20107634
λ_2 (µm)	0.37878260	0.39210520
λ_3 (µm)	46.994595	47.047590
No. of Wavelengths	33	38
Wavelength Range (µm)	0.54-18.2	0.54-18.2
Average Absolute Residual of n (10^{-5})	6.2	4.1

Table 2a. Refractive Index of Commercial KCl at Discrete Wavelengths (T = 19.9 °C).

λ (μm)	n	λ (μm)	n	λ (μm)	n
0.25	1.59010	0.95	1.48019	7.50	1.46459
0.30	1.54574	1.00	1.47959	8.00	1.46319
0.35	1.52365	1.50	1.47642	8.50	1.46169
0.40	1.51072	2.00	1.47508	9.00	1.46010
0.45	1.50240	2.50	1.47422	9.50	1.45842
0.50	1.49670	3.00	1.47348	10.00	1.45664
0.55	1.49260	3.50	1.47275	10.50	1.45477
0.60	1.48955	4.00	1.47199	11.00	1.45280
0.65	1.48721	4.50	1.47117	11.50	1.45073
0.70	1.48537	5.00	1.47028	12.00	1.44856
0.75	1.48390	5.50	1.46931	12.50	1.44629
0.80	1.48271	6.00	1.46826	13.00	1.44391
0.85	1.48172	6.50	1.46712	13.50	1.44143
0.90	1.48089	7.00	1.46590	14.00	1.43885

Table 2b. Refractive Index of RAP KCl at Discrete Wavelengths (T = 20.2 °C).

λ (μm)	n	λ (μm)	n	λ (μm)	n
0.25	1.59029	1.00	1.47961	8.50	1.46169
0.30	1.54577	1.50	1.47643	9.00	1.46009
0.35	1.52367	2.00	1.47510	9.50	1.45839
0.40	1.51075	2.50	1.47424	10.00	1.45658
0.45	1.50243	3.00	1.47350	10.50	1.45467
0.50	1.49673	3.50	1.47278	11.00	1.45266
0.55	1.49263	4.00	1.47202	11.50	1.45054
0.60	1.48957	4.50	1.47120	12.00	1.44831
0.65	1.48723	5.00	1.47031	12.50	1.44597
0.70	1.48540	5.50	1.46934	13.00	1.44352
0.75	1.48392	6.00	1.46829	13.50	1.44095
0.80	1.48273	6.50	1.46716	14.00	1.43826
0.85	1.48174	7.00	1.46593	14.50	1.43545
0.90	1.48091	7.50	1.46461	15.00	1.43252
0.95	1.48021	8.00	1.46320	15.50	1.42946

Table 2c. Refractive Index of KCl:KI (1.5% KI) at Discrete Wavelengths (T = 19.9 °C).

λ (μm)	n	λ (μm)	n	λ (μm)	n
0.25	1.59146	1.00	1.48019	8.50	1.46226
0.30	1.54669	1.50	1.47700	9.00	1.46066
0.35	1.52445	2.00	1.47567	9.50	1.45895
0.40	1.51146	2.50	1.47480	10.00	1.45715
0.45	1.50310	3.00	1.47406	10.50	1.45524
0.50	1.49737	3.50	1.47334	11.00	1.45323
0.55	1.49326	4.00	1.47258	11.50	1.45112
0.60	1.49019	4.50	1.47176	12.00	1.44889
0.65	1.48784	5.00	1.47087	12.50	1.44656
0.70	1.48599	5.50	1.46991	13.00	1.44411
0.75	1.48452	6.00	1.46886	13.50	1.44154
0.80	1.48332	6.50	1.46772	14.00	1.43886
0.85	1.48232	7.00	1.46649	14.50	1.43605
0.90	1.48149	7.50	1.46518	15.00	1.43312
0.95	1.48079	8.00	1.46377	15.50	1.43006

Table .2d. Refractive Index of Hot Forged CaF$_2$ at Discrete Wavelengths (T = 20.8 °C).

λ (μm)	n	λ (μm)	n	λ (μm)	n
0.25	1.46730	0.75	1.43112	3.50	1.41402
0.30	1.45399	0.80	1.43055	4.00	1.40961
0.35	1.44652	0.85	1.43006	4.50	1.40458
0.40	1.44185	0.90	1.42963	5.00	1.39891
0.45	1.43872	0.95	1.42925	5.50	1.39258
0.50	1.43649	1.00	1.42890	6.00	1.38556
0.55	1.43485	1.50	1.42627	6.50	1.37782
0.60	1.43358	2.00	1.42386	7.00	1.36933
0.65	1.43259	2.50	1.42110	7.50	1.36005
0.70	1.43178	3.00	1.41784	8.00	1.34995

Table 2e. Refractive Index of Fusion Cast CaF$_2$ at Discrete Wavelengths (T = 21.7 °C).

λ (μm)	n	λ (μm)	n	λ (μm)	n
0.25	1.46728	0.80	1.43054	4.50	1.40464
0.30	1.45401	0.85	1.43006	5.00	1.39897
0.35	1.44652	0.90	1.42963	5.50	1.39264
0.40	1.44184	0.95	1.42925	6.00	1.38561
0.45	1.43870	1.00	1.42890	6.50	1.37786
0.50	1.43647	1.50	1.42628	7.00	1.36934
0.55	1.43483	2.00	1.42388	7.50	1.36003
0.60	1.43357	2.50	1.42112	8.00	1.34987
0.65	1.43257	3.00	1.41787	8.50	1.33881
0.70	1.43177	3.50	1.41406		
0.75	1.43111	4.00	1.40966		

Table 2f. Refractive Index of Fusion Cast SrF$_2$ at Discrete Wavelengths (T = 20.0 °C).

λ (μm)	n	λ (μm)	n	λ (μm)	n
0.25	1.47336	0.90	1.43382	6.50	1.39941
0.30	1.45922	0.95	1.43346	7.00	1.39402
0.35	1.45131	1.00	1.43314	7.50	1.38816
0.40	1.44639	1.50	1.43095	8.00	1.38180
0.45	1.44309	2.00	1.42922	8.50	1.37493
0.50	1.44077	2.50	1.42734	9.00	1.36752
0.55	1.43906	3.00	1.42519	9.50	1.35955
0.60	1.43776	3.50	1.42269	10.00	1.35099
0.65	1.43675	4.00	1.41982	10.50	1.34181
0.70	1.43593	4.50	1.41657	11.00	1.33198
0.75	1.43527	5.00	1.41291	11.50	1.32146
0.80	1.43471	5.50	1.40884		
0.85	1.43423	6.00	1.40435		

Table 2g. Refractive Index of CVD ZnS Specimen #1 at Discrete Wavelengths (T = 21.6 °C).

λ (μm)	n	λ (μm)	n	λ (μm)	n
0.55	2.38579	1.50	2.27209	6.50	2.23583
0.60	2.36237	2.00	2.26453	7.00	2.23183
0.65	2.34509	2.50	2.26030	7.50	2.22749
0.70	2.33189	3.00	2.25719	8.00	2.22280
0.75	2.32155	3.50	2.25445	8.50	2.21775
0.80	2.31327	4.00	2.25178	9.00	2.21231
0.85	2.30652	4.50	2.24903	9.50	2.20645
0.90	2.30093	5.00	2.24610	10.00	2.20016
0.95	2.29626	5.50	2.24294	10.50	2.19340
1.00	2.29230	6.00	2.23953		

Table 2h. Refractive Index of CVD ZnS Specimen #2 at Discrete Wavelengths (T = 21.9 °C).

λ (μm)	n	λ (μm)	n	λ (μm)	n
0.55	2.38579	1.50	2.27206	6.50	2.23595
0.60	2.36232	2.00	2.26451	7.00	2.23196
0.65	2.34503	2.50	2.26029	7.50	2.22763
0.70	2.33184	3.00	2.25719	8.00	2.22296
0.75	2.32150	3.50	2.25447	8.50	2.21791
0.80	2.31322	4.00	2.25182	9.00	2.21246
0.85	2.30647	4.50	2.24907	9.50	2.20660
0.90	2.30089	5.00	2.24616	10.00	2.20029
0.95	2.29622	5.50	2.24303	10.50	2.19351
1.00	2.29226	6.00	2.23963		

Table 2i. Refractive Index of CVD ZnSe Specimen #1 at Discrete Wavelengths (T = 20.3 °C).

λ (μm)	n	λ (μm)	n	λ (μm)	n
0.55	2.66246	4.00	2.43316	11.50	2.39650
0.60	2.61380	4.50	2.43132	12.00	2.39281
0.65	2.58054	5.00	2.42953	12.50	2.38892
0.70	2.55636	5.50	2.42772	13.00	2.38481
0.75	2.53804	6.00	2.42584	13.50	2.38048
0.80	2.52373	6.50	2.42388	14.00	2.37593
0.85	2.51230	7.00	2.42181	14.50	2.37114
0.90	2.50298	7.50	2.41961	15.00	2.36610
0.95	2.49528	8.00	2.41728	15.50	2.36080
1.00	2.48882	8.50	2.41481	16.00	2.35523
1.50	2.45708	9.00	2.41218	16.50	2.34937
2.00	2.44620	9.50	2.40939	17.00	2.34322
2.50	2.44087	10.00	2.40644	17.50	2.33675
3.00	2.43758	10.50	2.40331	18.00	2.32996
3.50	2.43517	11.00	2.40000		

Table 2j. Refractive Index of CVD ZnSe Specimen #2 at Discrete Wavelengths (T = 20.8 °C).

λ (μm)	n	λ (μm)	n	λ (μm)	n
0.55	2.66278	4.00	2.43312	11.50	2.39666
0.60	2.61409	4.50	2.43128	12.00	2.39299
0.65	2.58090	5.00	2.42949	12.50	2.38913
0.70	2.55676	5.50	2.42769	13.00	2.38505
0.75	2.53846	6.00	2.42582	13.50	2.38075
0.80	2.52415	6.50	2.42387	14.00	2.37623
0.85	2.51270	7.00	2.42181	14.50	2.37148
0.90	2.50336	7.50	2.41962	15.00	2.36647
0.95	2.49563	8.00	2.41731	15.50	2.36121
1.00	2.48915	8.50	2.41485	16.00	2.35568
1.50	2.45721	9.00	2.41224	16.50	2.34987
2.00	2.44624	9.50	2.40947	17.00	2.34376
2.50	2.44086	10.00	2.40653	17.50	2.33735
3.00	2.43755	10.50	2.40342	18.00	2.33060
3.50	2.43513	11.00	2.40014		

Table 2k. Change in Refractive Index of CaF$_2$:Er with Increase in Percentage of Er.

λ (μm)	n Hot-Forged CaF$_2$	n CaF$_2$(A) [a]	Δn x 10^5							
			A-HF	B-A	C-B	D-C	E-D	F-E	G-F	H-G
0.4047	1.441509	1.441506	-0.3	2.6	1.0	4.5	14.4	43.9	160.5	478.3
0.4358	1.439492	1.439493	0.1	1.9	1.2	4.4	14.7	43.8	158.5	477.4
0.4678	1.437840	1.437841	0.1	1.7	1.4	4.3	14.4	43.7	158.3	475.0
0.4800	1.437297	1.437301	0.4	1.6	0.9	4.2	14.8	43.5	157.4	473.9
0.5086	1.436170	1.436174	0.4	1.2	1.3	4.4	15.0	43.6	157.2	472.0
0.5461	1.434959	1.434957	-0.2	1.6	1.3	4.2	15.3	42.7	156.8	471.3
0.5876	--	1.433867	--	1.8	1.2	4.2	15.2	42.5	156.8	469.7
0.6438	1.432701	1.432699	-0.2	1.7	1.6	3.8	14.6	43.4	155.5	466.9
0.6678	--	1.432297	--	0.5	1.3	3.8	15.8	42.1	156.0	468.5
0.7065	--	1.431703	--	1.2	1.3	3.7	15.2	41.9	158.0	463.4
1.014	1.428811	1.428823	1.2	1.7	1.5	4.8	15.6	39.6	156.0	462.1
1.083	1.428384	1.428400	1.6	1.6	1.2	3.3	15.7	41.8	155.2	460.7
AVG Δnx10^5	--	--	0.47	1.59	1.27	4.13	15.06	42.70	157.18	469.93

[a] HF=hot forged; A=.001% Er; B=.003% Er; C=.01% Er; D=.03% Er; E=.1% Er; F=.3% Er; G=1% Er; H=3% Er.

Table 3. Linear Thermal Expansion Coefficients ($10^{-6} \mathrm{K}^{-1}$)

Temperature (°C)	Materials						
	BaF_2	CdF_2	CaF_2	KBr	KCl	LiF	NaF
-180	9.1	9.9	6.7	28.5	24.5	8.4	12.3
-160	11.2	12.3	9.1	30.9	27.3	12.7	16.6
-140	12.8	14.2	11.1	32.5	29.1	16.8	20.2
-120	14.1	15.6	12.8	33.8	30.5	20.4	23.1
-100	15.1	16.8	14.1	34.9	31.8	23.4	25.4
-80	15.9	17.8	15.2	35.9	33.0	26.0	27.2
-60	16.5	18.7	16.2	36.6	34.1	28.1	28.6
-40	17.0	19.4	17.0	37.2	35.0	29.8	29.7
-20	17.5	20.1	17.7	37.7	35.8	31.2	30.7
0	17.9	20.7	18.3	38.2	36.5	32.3	31.5
20	18.4	21.3	18.7	38.7	37.1	33.2	32.2
40	18.8	21.8	19.1	39.2	37.7	34.1	32.9
60	19.2	22.2	19.4	39.6	38.3	34.8	33.5
80	19.5	22.7	19.7	40.1	38.8	35.6	34.1
100	19.8	23.2	20.0	40.4	39.4	36.4	34.7
120	20.1	23.7	20.4	40.8	39.8	37.2	35.2
140	20.4	24.2	20.8	41.2	40.3	38.0	35.8
160	20.8	24.8	21.3	41.7	40.9	38.8	36.3
180	21.1	25.3	21.7	42.4	41.5	39.5	36.9
200	21.4	25.9	22.2	42.8	41.9	40.4	37.4

Table 3. Linear Thermal Expansion Coefficients ($10^{-6} K^{-1}$) (continued)

Temperature (°C)	Materials						
	SrF_2	ZnS	ZnSe	Al_2O_3 ⊥c-axis	MgF_2 ⊥c-axis	MgF_2 ‖c-axis	NaCl
-180	7.7	1.2	2.6	0.34	0.72	2.90	23.6
-160	10.0	2.2	3.7	0.69	1.63	4.45	27.7
-140	11.8	3.1	4.6	1.14	2.65	5.95	30.8
-120	13.3	3.9	5.2	1.65	3.64	7.39	32.9
-100	14.4	4.6	5.6	2.19	4.58	8.86	34.4
-80	15.3	5.1	6.0	2.73	5.45	9.82	35.5
-60	16.1	5.5	6.4	3.24	6.23	10.86	36.4
-40	16.7	5.9	6.7	3.73	6.93	11.74	37.3
-20	17.2	6.3	6.9	4.18	7.52	12.47	38.1
0	17.6	6.6	7.1	4.60	8.04	13.07	38.9
20	17.9	6.8	7.3	4.99	8.48	13.70	39.6
40	18.2	7.0	7.5	5.34	8.88	14.09	40.2
60	18.4	7.2	7.6	5.66	9.25	14.54	40.8
80	18.7	7.3	7.7	5.95	9.60	14.94	41.3
100	18.9	7.3	7.8	6.20	9.93	15.32	41.9
120	19.1	7.4	7.9	6.42	10.22	15.67	42.5
140	19.4	7.4	8.0	6.61	10.49	16.00	43.0
160	19.6	7.5	8.1	6.79	10.71	16.33	43.4
180	19.9	7.6	8.2	6.95	10.91	16.67	43.8
200	20.2	7.7	8.3	7.10	11.10	17.00	44.4

41

Table 4a. dn/dT of Al_2O_3 (10^{-5} K^{-1})

Temperature (°C)	Wavelength (µm)	
	0.4579	
	dn_e/dT	dn_o/dT
-180	0.19	0.18
-160	0.36	0.32
-140	0.51	0.45
-120	0.65	0.58
-100	0.78	0.69
-80	0.89	0.79
-60	0.99	0.88
-40	1.07	0.96
-20	1.15	1.04
0	1.22	1.11
20	1.28	1.17
40	1.33	1.23
60	1.38	1.28
80	1.42	1.32
100	1.47	1.37
120	1.51	1.41
140	1.55	1.44
160	1.59	1.48
180	1.64	1.51
200	1.69	1.54
σ^a	0.04	0.03

[a]Standard deviation from a third degree polynomial fit.

Table 4b. dn/dT of BaF$_2$ (10^{-5} K^{-1})

Temperature (°C)	Wavelength (µm)				
	0.4579	0.6328	1.15	3.39	10.6
-180	-0.78	-0.86	-0.81	-0.81	-0.73
-160	-0.92	-0.98	-0.96	-0.95	-0.85
-140	-1.04	-1.09	-1.08	-1.07	-0.96
-120	-1.15	-1.19	-1.19	-1.17	-1.05
-100	-1.24	-1.27	-1.29	-1.26	-1.13
- 80	-1.32	-1.35	-1.37	-1.34	-1.21
- 60	-1.38	-1.41	-1.44	-1.41	-1.27
- 40	-1.44	-1.47	-1.50	-1.47	-1.32
- 20	-1.49	-1.52	-1.55	-1.51	-1.37
0	-1.53	-1.56	-1.59	-1.56	-1.41
20	-1.56	-1.60	-1.62	-1.59	-1.45
40	-1.60	-1.63	-1.66	-1.62	-1.48
60	-1.63	-1.66	-1.69	-1.66	-1.51
80	-1.65	-1.70	-1.71	-1.68	-1.54
100	-1.68	-1.73	-1.74	-1.71	-1.57
120	-1.71	-1.76	-1.77	-1.75	-1.60
140	-1.75	-1.79	-1.80	-1.78	-1.63
160	-1.78	-1.83	-1.84	-1.82	-1.66
180	-1.83	-1.87	-1.88	-1.87	-1.70
200	-1.88	-1.92	-1.93	-1.92	-1.75
σ[a]	0.03	0.02	0.03	0.03	0.03

[a]Standard deviation from a third degree polynomial fit.

Table 4c. dn/dT of CaF_2 (10^{-5} K^{-1})

Temperature (°C)	Wavelength (µm)			
	0.4579	0.6328	1.15	3.39
-180	-0.39	-0.40	-0.41	-0.40
-160	-0.53	-0.54	-0.56	-0.52
-140	-0.64	-0.66	-0.68	-0.63
-120	-0.74	-0.77	-0.78	-0.73
-100	-0.83	-0.85	-0.87	-0.82
- 80	-0.90	-0.93	-0.95	-0.89
- 60	-0.95	-0.99	-1.01	-0.95
- 40	-1.00	-1.03	-1.06	-1.00
- 20	-1.04	-1.07	-1.10	-1.05
0	-1.07	-1.10	-1.13	-1.09
20	-1.10	-1.13	-1.15	-1.12
40	-1.12	-1.15	-1.18	-1.14
60	-1.14	-1.17	-1.20	-1.17
80	-1.16	-1.19	-1.22	-1.19
100	-1.18	-1.21	-1.24	-1.21
120	-1.20	-1.23	-1.26	-1.23
140	-1.22	-1.26	-1.29	-1.25
160	-1.26	-1.30	-1.32	-1.27
180	-1.29	-1.34	-1.36	-1.30
200	-1.34	-1.40	-1.41	-1.34
σ[a]	0.01	0.02	0.02	0.03

[a]Standard deviation from a third degree polynomial fit.

Table 4d. dn/dT of CdF_2 $(10^{-5} \, K^{-1})$

Temperature (°C)	Wavelength (µm)			
	0.4579	0.6328	1.15	3.39
-180	-0.43	-0.56	-0.57	-0.53
-160	-0.52	-0.64	-0.67	-0.64
-140	-0.59	-0.72	-0.76	-0.73
-120	-0.65	-0.75	-0.83	-0.81
-100	-0.71	-0.84	-0.90	-0.87
- 80	-0.75	-0.89	-0.96	-0.93
- 60	-0.80	-0.93	-1.00	-0.98
- 40	-0.83	-0.97	-1.05	-1.02
- 20	-0.86	-1.01	-1.08	-1.05
0	-0.89	-1.04	-1.12	-1.08
20	-0.92	-1.07	-1.15	-1.11
40	-0.94	-1.10	-1.17	-1.14
60	-0.97	-1.13	-1.20	-1.17
80	-1.00	-1.16	-1.23	-1.20
100	-1.02	-1.19	-1.27	-1.23
120	-1.06	-1.23	-1.30	-1.27
140	-1.09	-1.27	-1.34	-1.31
160	-1.14	-1.31	-1.39	-1.36
180	-1.18	-1.37	-1.44	-1.42
200	-1.24	-1.43	-1.51	-1.49
σ^a	0.02	0.02	0.02	0.04

[a]Standard deviation from a third degree polynomial fit.

Table 4e. dn/dT of KBr (10^{-5} K^{-1})

Temperature (°C)	Wavelength (µm)				
	0.4579	0.6328	1.15	3.39	10.6
-180	-2.85	-2.95	-3.05	-3.05	-3.06
-160	-3.30	-3.17	-3.26	-3.26	-3.24
-140	-3.19	-3.36	-3.44	-3.44	-3.40
-120	-3.33	-3.53	-3.59	-3.60	-3.54
-100	-3.46	-3.67	-3.73	-3.74	-3.66
- 80	-3.56	-3.78	-3.84	-3.85	-3.77
- 60	-3.66	-3.88	-3.94	-3.95	-3.86
- 40	-3.74	-3.96	-4.02	-4.03	-3.93
- 20	-3.81	-4.02	-4.09	-4.10	-4.00
0	-3.88	-4.08	-4.14	-4.16	-4.06
20	-3.93	-4.12	-4.19	-4.21	-4.11
40	-3.98	-4.16	-4.23	-4.25	-4.16
60	-4.03	-4.19	-4.27	-4.29	-4.20
80	-4.07	-4.23	-4.31	-4.33	-4.25
100	-4.11	-4.27	-4.35	-4.36	-4.29
120	-4.16	-4.31	-4.39	-4.40	-4.33
140	-4.20	-4.36	-4.44	-4.44	-4.38
160	-4.25	-4.42	-4.49	-4.49	-4.43
180	-4.31	-4.49	-4.56	-4.55	-4.49
200	-4.38	-4.58	-4.63	-4.62	-4.56
σ^a	0.04	0.03	0.03	0.03	0.06

[a] Standard deviation from a third degree polynomial fit.

Table 4f. dn/dT of KCl (10^{-5} K^{-1})

Temperature (°C)	Wavelength (μm)				
	0.4579	0.6328	1.15	3.39	10.6
-180	-2.26	-2.32	-2.35	-2.39	-2.33
-160	-2.44	-2.52	-2.55	-2.58	-2.50
-140	-2.61	-2.70	-2.74	-2.75	-2.65
-120	-2.76	-2.86	-2.90	-2.91	-2.80
-100	-2.90	-3.00	-3.05	-3.05	-2.93
- 80	-3.02	-3.13	-3.17	-3.17	-3.04
- 60	-3.14	-3.24	-3.29	-3.28	-3.15
- 40	-3.24	-3.35	-3.39	-3.38	-3.24
- 20	-3.33	-3.43	-3.48	-3.47	-3.33
0	-3.41	-3.51	-3.55	-3.55	-3.41
20	-3.49	-3.58	-3.62	-3.62	-3.48
40	-3.55	-3.65	-3.68	-3.69	-3.54
60	-3.61	-3.70	-3.74	-3.75	-3.60
80	-3.67	-3.76	-3.79	-3.80	-3.65
100	-3.72	-3.81	-3.84	-3.85	-3.70
120	-3.77	-3.86	-3.89	-3.90	-3.74
140	-3.82	-3.91	-3.94	-3.94	-3.79
160	-3.87	-3.96	-4.00	-3.99	-3.83
180	-3.91	-4.02	-4.05	-4.04	-3.87
200	-3.96	-4.08	-4.11	-4.09	-3.91
σ^a	0.02	0.02	0.02	0.02	0.04

[a]Standard deviation from a third degree polynomial fit.

Table 4g. dn/dT of LiF (10^{-5} K^{-1})

Temperature (°C)	Wavelength (μm)			
	0.4579	0.6328	1.15	3.39
-180	-0.33	-0.36	-0.38	-0.40
-160	-0.61	-0.63	-0.64	-0.60
-140	-0.85	-0.86	-0.86	-0.78
-120	-1.04	-1.05	-1.05	-0.93
-100	-1.20	-1.21	-1.21	-1.06
- 80	-1.32	-1.34	-1.34	-1.16
- 60	-1.42	-1.44	-1.45	-1.25
- 40	-1.49	-1.52	-1.53	-1.32
- 20	-1.54	-1.59	-1.60	-1.37
0	-1.58	-1.63	-1.65	-1.42
20	-1.60	-1.67	-1.69	-1.45
40	-1.63	-1.70	-1.73	-1.48
60	-1.65	-1.72	-1.75	-1.51
80	-1.67	-1.75	-1.77	-1.53
100	-1.71	-1.78	-1.79	-1.56
120	-1.75	-1.81	-1.81	-1.59
140	-1.82	-1.85	-1.84	-1.63
160	-1.90	-1.91	-1.88	-1.67
180	-2.02	-1.99	-1.92	-1.73
200	-2.16	-2.09	-1.99	-1.80
σ^a	0.03	0.02	0.04	0.04

Table 4h. dn/dT of MgF_2 (10^{-5} K^{-1})

Temperature (°C)	0.4579		0.6328		1.15		3.39	
	Wavelength (μm)							
	dn_e/dT	dn_o/dT	dn_e/dT	dn_o/dT	dn_e/dT	dn_o/dT	dn_e/dT	dn_o/dT
-180	0.177	0.244	0.165	0.223	0.144	0.199	0.15	0.20
-160	0.168	0.234	0.154	0.212	0.133	0.188	0.14	0.20
-140	0.159	0.225	0.144	0.201	0.122	0.177	0.13	0.19
-120	0.151	0.215	0.133	0.190	0.110	0.166	0.12	0.18
-100	0.142	0.205	0.122	0.179	0.099	0.155	0.12	0.17
- 80	0.133	0.196	0.112	0.168	0.088	0.144	0.11	0.16
- 60	0.124	0.186	0.101	0.157	0.077	0.132	0.10	0.15
- 40	0.116	0.176	0.090	0.146	0.065	0.121	0.09	0.14
- 20	0.107	0.166	0.080	0.135	0.054	0.110	0.08	0.13
0	0.098	0.157	0.069	0.124	0.043	0.099	0.07	0.12
20	0.089	0.147	0.058	0.112	0.032	0.088	0.06	0.11
40	0.081	0.137	0.048	0.101	0.020	0.077	0.05	0.10
60	0.072	0.128	0.037	0.090	0.009	0.066	0.04	0.10
80	0.063	0.118	0.027	0.079	-0.002	0.054	0.03	0.09
100	0.054	0.108	0.016	0.068	-0.013	0.043	0.02	0.08
120	0.046	0.099	0.005	0.057	-0.025	0.032	0.01	0.07
140	0.037	0.089	-0.005	0.046	-0.036	0.021	0	0.06
160	0.028	0.079	-0.016	0.035	-0.047	0.010	-0.01	0.05
180	0.019	0.070	-0.027	0.024	-0.059	-0.001	-0.02	0.04
200	0.011	0.060	-0.037	0.013	-0.070	-0.013	-0.03	0.03
σ^a	0.009	0.014	0.009	0.012	0.010	0.014	0.02	0.01

[a]Standard deviation from linear fit.

49

Table 4i. dn/dT of NaCl (10^{-5} K^{-1})

Temperature (°C)	Wavelength (µm)			
	0.4579	0.6328	1.15	3.39
−180	−2.06	−2.16	−2.22	−2.24
−160	−2.30	−2.40	−2.48	−2.49
−140	−2.51	−2.61	−2.70	−2.70
−120	−2.69	−2.79	−2.89	−2.89
−100	−2.85	−2.96	−3.06	−3.05
− 80	−2.99	−3.09	−3.20	−3.19
− 60	−3.11	−3.21	−3.32	−3.31
− 40	−3.30	−3.32	−3.42	−3.41
− 20	−3.29	−3.40	−3.51	−3.49
0	−3.36	−3.48	−3.58	−3.57
20	−3.42	−3.54	−3.64	−3.63
40	−3.48	−3.60	−3.70	−3.68
60	−3.53	−3.65	−3.74	−3.73
80	−3.57	−3.69	−3.79	−3.78
100	−3.62	−3.74	−3.83	−3.83
120	−3.67	−3.78	−3.88	−3.88
140	−3.72	−3.83	−3.93	−3.94
160	−3.78	−3.88	−3.99	−4.01
180	−3.84	−3.94	−4.06	−4.09
200	−3.92	−4.01	−4.14	−4.18
σ^a	0.05	0.04	0.04	0.04

[a]Standard deviation from a third degree polynomial fit.

Table 4j. dn/dT of NaF (10^{-5} K^{-1})

Temperature (°C)	Wavelength (µm)			
	0.4579	0.6328	1.15	3.39
-180	-0.41	-0.42	-0.45	-0.45
-160	-0.55	-0.59	-0.63	-0.61
-140	-0.68	-0.74	-0.78	-0.75
-120	-0.79	-0.86	-0.91	-0.86
-100	-0.88	-0.96	-1.02	-0.96
- 80	-0.96	-1.05	-1.10	-1.04
- 60	-1.02	-1.12	-1.17	-1.11
- 40	-1.08	-1.17	-1.23	-1.16
- 20	-1.12	-1.22	-1.27	-1.20
0	-1.16	-1.25	-1.30	-1.23
20	-1.19	-1.28	-1.32	-1.25
40	-1.22	-1.30	-1.34	-1.27
60	-1.24	-1.32	-1.36	-1.29
80	-1.27	-1.33	-1.37	-1.31
100	-1.29	-1.35	-1.39	-1.32
120	-1.31	-1.37	-1.41	-1.34
140	-1.34	-1.40	-1.44	-1.37
160	-1.38	-1.43	-1.48	-1.40
180	-1.42	-1.47	-1.53	-1.44
200	-1.47	-1.52	-1.59	-1.49
σ[a]	0.02	0.05	0.05	0.05

[a]Standard deviation from a third degree polynomial fit.

Table 4k. dn/dT of SrF$_2$ (10^{-5} K^{-1})

Temperature (°C)	Wavelength (µm)				
	0.4579	0.6328	1.15	3.39	10.6
−180	−0.54	−0.56	−0.55	−0.56	−0.35
−160	−0.67	−0.69	−0.69	−0.68	−0.49
−140	−0.77	−0.81	−0.81	−0.80	−0.61
−120	−0.86	−0.90	−0.91	−0.89	−0.71
−100	−0.94	−0.98	−1.00	−0.97	−0.79
− 80	−1.01	−1.05	−1.07	−1.04	−0.85
− 60	−1.06	−1.11	−1.13	−1.10	−0.90
− 40	−1.11	−1.15	−1.17	−1.15	−0.93
− 20	−1.15	−1.19	−1.21	−1.19	−0.96
0	−1.18	−1.22	−1.24	−1.22	−0.97
20	−1.20	−1.24	−1.26	−1.24	−0.98
40	−1.22	−1.25	−1.28	−1.26	−0.99
60	−1.24	−1.27	−1.29	−1.27	−0.99
80	−1.25	−1.28	−1.30	−1.28	−1.00
100	−1.26	−1.29	−1.31	−1.29	−1.01
120	−1.27	−1.30	−1.32	−1.29	−1.02
140	−1.29	−1.32	−1.33	−1.30	−1.05
160	−1.30	−1.34	−1.35	−1.31	−1.08
180	−1.32	−1.36	−1.37	−1.32	−1.13
200	−1.34	−1.39	−1.40	−1.33	−1.20
σ[a]	0.03	0.02	0.01	0.03	0.05

[a]Standard deviation from a third degree polynomial fit.

Table 4ℓ. dn/dT of CVD ZnS (10^{-5} K^{-1})

Temperature (°C)	Wavelength (µm)		
	1.15	3.39	10.6
-180	3.5	2.8	2.7
-160	3.7	3.1	3.0
-140	3.8	3.3	3.3
-120	4.0	3.5	3.5
-100	4.1	3.7	3.7
- 80	4.2	3.9	3.8
- 60	4.3	4.0	3.9
- 40	4.4	4.1	4.0
- 20	4.5	4.1	4.0
0	4.5	4.2	4.1
20	4.6	4.2	4.1
40	4.6	4.3	4.1
60	4.7	4.3	4.1
80	4.7	4.3	4.1
100	4.7	4.3	4.2
120	4.8	4.4	4.2
140	4.8	4.4	4.3
160	4.9	4.4	4.4
180	4.9	4.5	4.5
200	5.0	4.6	4.7
σ^a	0.2	0.2	0.2

[a]Standard deviation from a third degree polynomial fit.

Table 4m. dn/dT of CVD ZnSe (10^{-5} K^{-1})

Temperature (°C)	Wavelength (μm)			
	0.6328	1.15	3.39	10.6
-180	7.6	5.4	5.0	4.9
-160	8.2	5.7	5.2	5.1
-140	8.7	6.0	5.4	5.4
-120	9.1	6.3	5.6	5.5
-100	9.4	6.5	5.8	5.7
- 80	9.7	6.6	5.9	5.8
- 60	10.0	6.7	6.0	5.9
- 40	10.2	6.8	6.1	6.0
- 20	10.3	6.9	6.1	6.0
0	10.5	7.0	6.2	6.1
20	10.6	7.0	6.2	6.1
40	10.7	7.0	6.2	6.1
60	10.8	7.1	6.3	6.1
80	10.9	7.1	6.3	6.2
100	11.0	7.2	6.3	6.2
120	11.1	7.2	6.4	6.3
140	11.3	7.3	6.4	6.3
160	11.5	7.4	6.5	6.4
180	11.8	7.6	6.6	6.6
200	12.1	7.8	6.7	6.7
σ^{a}	0.1	0.1	0.1	0.1

[a]Standard deviation from a third degree polynomial fit.

Table 5. Data Used for Computing dn/dT

Material	Refractive Index					t_o (mm)
	λ = 0.4579 μm	0.6328 μm	1.15 μm	3.39 μm	10.6 μm	
Al_2O_3[a] $\quad n_o$	1.779					9.55
$\quad\quad\quad n_e$	1.770					--
BaF_2[a]	1.480	1.473	1.468	1.460	1.393	13.16
CaF_2[a]	1.438	1.433	1.428	1.415	--	13.41
CdF_2[a]	1.585[b]	1.574[b]	1.55[c]	1.54[c]	--	7.33
KBr[a]	1.577	1.557	1.542	1.536	1.525	11.83
KCl[a]	1.502	1.488	1.478	1.473	1.454	11.87
LiF[a]	1.396	1.392	1.386	1.360	--	5.59
MgF_2[a] $\quad n_o$	1.381	1.377	1.373	1.358	--	13.40
$\quad\quad\quad n_e$	1.393	1.389	1.384	1.369	--	--
$NaCl$[a]	1.558	1.542	1.531	1.524	--	--
NaF[a]	1.329	1.325	1.321	1.312	--	12.21
SrF_2	1.443	1.437	1.432	1.423	1.340	13.15
ZnS (CVD)	--	--	2.283	2.255	2.192	4.47
ZnSe (CVD)	--	2.591	2.475	2.436	2.403	17.49

[a] See American Institute of Physics Handbook (McGraw-Hill, 1972) pp. 6-12 or Handbook of Optics, Eds. W. G. Driscoll and W. Vaughan (McGraw-Hill, 1978) pp. 7-1.

[b] B. Krukowska-Fulde and T. Niemski, J. Crystl. Growth 1, 183 (1967).

[c] Estimated.

Table 6. Piezo-Optic Constants, q_{11} and q_{12}, and Elastic Compliance, s_{12}, of As_2S_3 Glass and a Chalcogenide Glass in Units of $10^{-12} Pa^{-1}$

	n [a]	q_{11} [b]	q_{12} [b]	$q_{12}-q_{11}$ [b]	s_{12} [b]
As_2S_3 Glass					
0.6328 μm	2.606	7.63	6.36	-1.27	-18.6, -18.8 [c]
1.15 μm	2.452	7.64	6.54	-1.10	
10.6 μm	2.354	8.23	6.95	-1.28	
Chalcogenide Glass (Ge 33%, As 12%, Se 55%)					
1.15 μm	2.5704	5.32	4.89	-0.43	-12.0, -12.2 [d]
10.6 μm	2.4919	5.42	4.94	-0.48	-11.5 [e]

[a] These values were not measured in this work but are given because they were used to calculate the q_{ij}.

[b] Estimated accuracy of numbers from this work is ±2%.

[c] F. W. Glaze, D. H. Blackburn, J. S. Osmalov, D. Hubbard, and Mason H. Black, J. Res. Natl. Bur. Std. 59, 83 (1957).

[d] Ray Hilton, private communication -- value from Texas Instruments.

[e] Ray Hilton, private communication -- value from Bell Laboratories.

Table 7a.   Piezo-optic Constants of Alkaline-Earth Fluorides* $(10^{-12}Pa^{-1})$

	$\lambda = 0.6378\ \mu m$	$\lambda = 1.15\ \mu m$	$\lambda = 3.39\ \mu m$
$\underline{CaF}_2$			
q_{11}	-0.38 ±0.03	-0.40 ±0.06	-0.52 ±0.11
q_{12}	1.08 ±0.03	1.09 ±0.06	1.00 ±0.11
$(q_{11}-q_{12})$	-1.46 ±0.01	-1.49 ±0.02	-1.51 ±0.03
q_{44}	0.71 ±0.01	0.72 ±0.01	0.87 ±0.06
$\underline{SrF}_2$			
q_{11}	-0.64 ±0.04	-0.63 ±0.05	0.83 ±0.09
q_{12}	1.45 ±0.04	1.50 ±0.06	1.23 ±0.07
$(q_{11}-q_{12})$	-2.08 ±0.01	-2.13 ±0.04	-2.05 ±0.06
q_{44}	0.60 ±0.01	0.62 ±0.02	0.72 ±0.04
$\underline{BaF}_2$			
q_{11}	-0.99 ±0.03	-0.91 ±0.07	-0.75 ±0.07
q_{12}	2.07 ±0.04	2.13 ±0.07	2.11 ±0.05
$(q_{11}-q_{12})$	-3.06 ±0.01	-3.03 ±0.02	-2.91 ±0.08
q_{44}	0.95 ±0.01	0.95 ±0.01	0.99 ±0.07

Table 7b. Comparison of Piezo-optic Data in the Visible Region for Alkaline-Earth Fluorides (10^{-12} Pa^{-1}).

	NBS	Literature
CaF_2		
q_{11}	-0.38	-0.29^a, -0.41^b
q_{12}	1.08	1.16^a, 1.04^b
$(q_{11}-q_{12})$	-1.46	-1.45^a, -1.45^b, -1.48^d, -1.44^e, -1.47^f
q_{44}	0.71	0.70^a, 0.89^b, 0.81^d
SrF_2		
q_{11}	-0.64	-0.58^c
q_{12}	1.45	1.77^c
$(q_{11}-q_{12})$	-2.08	-2.35^c
q_{44}	0.60	0.59^c
BaF_2		
q_{11}	-0.99	-0.62^b
q_{12}	2.07	2.31^b
$(q_{11}-q_{12})$	-3.06	-2.93^b
q_{44}	0.95	1.06^b

[a] F. Pockels, Lehrbuch der Kirstalloptik (B. G. Teubner, Leipzig und Berlin, 1906). (λ=0.5893 µm).

[b] K. V. Rao, T. S. Narasimhamurty, J. Phys. Chem. Solids 31, 876 (1970). (λ=0.5893 µm).

[c] O. V. Shakin, M. F. Bryzhina, V. V. Lemanov, Sov. Phys. Solid State 13, 3141 (1972). (λ=0.6328 µm).

[d] K. S. Iyengar, K. B. Bansigar, Current Science 27, 436 (1958). (λ=0.5890 µm).

[e] A. J. Michael, J. Opt. Soc. Am. 58, 889 (1968). (λ=0.5461 µm).

[f] V. G. Krishna Murty, Ph.D. Thesis (Osmania University, Hyderabad, India, 1964). (λ=0.5461 µm).

Table 8. Photoelastic Constants[a] of Ge.

	$\lambda = 3.39$ μm	$\lambda = 10.6$ μm
q_{11} (10^{-12}Pa^{-1})	-0.79	-0.84
q_{12} (10^{-12}Pa^{-1})	-0.51	-0.48
q_{44} (10^{-12}Pa^{-1})	-1.07	-1.09
p_{11}	-0.151, -0.158[b]	-0.154
p_{12}	-0.128, -0.132[b]	-0.126
p_{44}	-0.072, -0.074[b]	-0.073
n	4.037[c]	4.006[c]

[a]Estimated accuracy approximately 2%. To calculate the elasto-optic constants we used the elastic constants of H. J. McSkimin, J. Appl. Phys. 24, 988 (1953).

[b]D. K. Biegelsen and J. C. Zesch, Phys. Rev. B 14, 3578 (1976).

[c]H. W. Icenogle, B. C. Platt, and W. L. Wolfe, Appl. Optics 15, 2348 (1977).

Table 9a. Piezo-optic Constants of KCl (10^{-12} Pa^{-1}).

λ (μm)	q_{11}	q_{12}	q_{44}	$q_{11}-q_{12}$	Ref.
0.589			-4.22	1.67	a
0.589			-4.42	1.66	b
0.589			-4.94	1.47	c
0.480			--	1.42	d
0.589			-4.74	1.57	e
0.633			--	1.81	f
0.633	4.6 ±0.2	2.7 ±0.8	-3.9 ±0.8	1.7 ±0.4	
0.644	--	--	-4.4 ±0.2	1.9 ±0.4	
*0.633	4.6 ±0.2	2.8 ±0.2	-4.6 ±0.2	1.9 ±0.2	
*0.644			-4.'7 ±0.2	1.9 ±0.1	
10.6			--	2.0	g
10.6			-2.62	--	h
10.6	4.3 ±0.3	2.8 ±0.3	-3.4 ±0.4	1.8 ±0.4	
*10.6	4.2 ±0.2	2.6 ±0.2	-3.6 ±0.3	1.8 ±0.2	

*Nomially doped with 1.5% KI.

[a] F. Pockels, Lehrbuch der Kristalloptik (Teubner, Leipzig, 1906), p. 408.

[b] Bhagavantam and Y. Krishna Murty, Proc. Indian Acad. Sci. A46, 399 (1957).

[c] K. G. Bansigir and K. S. Iyengar, Proc. Phys. Soc. London 71B, 225 (1958).

[d] R. Srinivasan, Zeit, f. Physik 155, 281 (1959).

[e] K. V. Krishna Rao and V. G. Krishna Murty, Proc. Indian Acad. Sci. 64, 24 (1966).

[f] W. W. Wilkening, J. D. Friedman and C. A. Pitha in Third Conference on High-Power Infrared Laser Windows, 1973, AFCRL-TR-47-0085-I.

[g] C. S. Chen, J. P. Szcznesniak, and J. C. Corelli, J. Appl. Phys. 46, (1975).

[h] C. A. Pitha and J. D. Friedman, in Proceedings of the Fourth Annual Conference on Infrared Window Materials, 1974, compiled by C. R. Andrews and C. L. Strecker.

Table 9b.   Elasto-Optic Constants of KCl

λ (μm)	P_{11}	P_{12}	P_{44}	P_{12}/P_{11}	Ref.
.589			-0.0276		a
.589	0.215	0.159	-0.024	-0.74	b
.589	0.246	0.192	-0.0298	-0.78	c
.633	0.21	0.15	-0.026	-0.70	
.644			-0.029		
* .633	0.21	0.15	-0.031	-0.72	
* .644			-0.031		
10.6	0.20	0.15	-0.023	-0.76	
*10.6	0.19	0.14	-0.024	-0.71	

*Nominally doped with 1.5% KI.

[a] F. Pockels, Lehrbuch der Kristalloptik (Teubner, Leipzig, 1906), p. 480.

[b] K. S. Iyengar, Nature 176, 1119 (1955).

[c] K. V. Krishna Rao and V. G. Krishna Murty, Proc. Indian Acad. Sci. 64, 24 (1966).

Table 10. Photoelastic Constants[a] of Fused SiO_2

	λ = 0.6328 µm	1.15 µm	3.39 µm
$q_{11}(10^{-12}Pa^{-1})$	0.42 ±0.01	0.58 ±0.01	0.81 ±0.01
$q_{12}(10^{-12}Pa^{-1})$	2.70 ±0.01	2.80 ±0.03	2.78 ±0.02
p_{11}	0.120 ±0.001	0.136 ±0.002	0.154 ±0.001
p_{12}	0.269 ±0.001	0.281 ±0.003	0.283 ±0.001
n	1.457	1.449	1.409

[a]The errors are based on the standard deviation of the data and do not take into account any errors in the elastic constants.

Table 11. Photoelastic Properties of CVD ZnSe

	λ = 0.6328 µm	λ = 10.6 µm
$q_{11}(10^{-12}Pa^{-1})$	-1.44 ±0.04, -1.48 ±0.05[a]	-1.46 ±0.07
$q_{12}(10^{-12}Pa^{-1})$	0.17 ±0.05, 0.22 ±0.05[a]	0.51 ±0.07
$q_{11}-q_{12}(10^{-12}Pa^{-1})$	-1.60 ±0.01	-1.97 ±0.02
p_{11}	-0.13	-0.10
p_{12}	-0.04	0.007

[a]L. F. Goldstein, J. S. Thompson, J. B. Schroeder and J. E. Slattery, Appl. Optics 14, 2432 (1975).

Table 12. Elastic Compliances Used in Computation of Piezo-Optic and Elasto-Optic Constants $(10^{-12} Pa^{-1})$.

	s_{11}	s_{12}	s_{44}	$s_{12}' = 1/3(s_{11}+2s_{12}-1/2\ s_{44})$
BaF_2[a]	15.126	-4.708	38.941	-4.587
CaF_2[a]	6.867	-1.451	29.764	-3.639
Ge[b]	9.75	-2.66	14.9	--
KCl[c]	25.8	-3.73	158.0	--
Fused SiO_2[d]	13.16	-2.16	--	--
SrF_2[a]	9.877	-2.553	31.969	-3.738
		-2.61[e]		-3.66[e]
ZnSe (CVD)	13.9 ±0.6[e]	-4.4 ±0.2[e]	--	--

[a] From tabulation by S. K. Dickinson, "Infrared Laser Window Materials Property Data for ZnSe, KCl, NaCl, CaF_2, SrF_2, BaF_2", Report No. AFCRL-TR-75-0318, PSRP # 635, Air Force Cambridge Research Laboratories, L. G. Hansom Field, Bedford, MA 01730 (1975).

[b] H. J. McSkimin, J. Appl. Phys. 24, 988 (1953).

[c] S. Haussül, Zeits. fur Physik 159, 223 (1960).

[d] W. Primak and D. Post, J. Appl. Phys. 30, 779 (1959).

[e] Obtained in this laboratory and used for calculating the piezo-optic constants.

U.S. DEPT. OF COMM. BIBLIOGRAPHIC DATA SHEET	1. PUBLICATION OR REPORT NO. TN 993	2. Gov't. Accession No.	3. Recipient's Accession No.

4. TITLE AND SUBTITLE	5. Publication Date
Optical Materials Characterization Final Technical Report February 1, 1978–September 30, 1978	February 1979
	6. Performing Organization Code

7. AUTHOR(S) Albert Feldman, Deane Horowitz, Roy M. Waxler, Marilyn J. Dodge	8. Performing Organ. Report No.

9. PERFORMING ORGANIZATION NAME AND ADDRESS	10. Project/Task/Work Unit No.
  NATIONAL BUREAU OF STANDARDS DEPARTMENT OF COMMERCE WASHINGTON, DC 20234	
	11. Contract/Grant No.

12. SPONSORING ORGANIZATION NAME AND COMPLETE ADDRESS (Street, City, State, ZIP)	13. Type of Report & Period Covered
Advanced Research Projects Agency Arlington, VA 22209	Final Technical Report 2/1/78 – 9/30/78
	14. Sponsoring Agency Code

15. SUPPLEMENTARY NOTES

☐ Document describes a computer program; SF-185, FIPS Software Summary, is attached.

16. ABSTRACT *(A 200-word or less factual summary of most significant information. If document includes a significant bibliography or literature survey, mention it here.)*

Data obtained as part of the Optical Materials Characterization Program are summarized in this report. Room temperature values of refractive index as a function of wavelength are presented for the following materials: commercially grown KCl, reactive atmosphere processed (RAP) KCl, KCl nominally doped with 1.5% KI, hot forged CaF_2, fusion cast CaF_2, CaF_2 doped with Er (0.001% to 3% Er), SrF_2, chemical vapor deposited (CVD) ZnSe (2 specimens), and ZnS (CVD, 2 specimens). Data for the thermo-optic constant (dn/dT) and the linear thermal expansion coefficient are given for the following materials over the temperature range −180 °C to 200 °C: Al_2O_3, BaF_2, CaF_2, CdF_2, KBr, KCl, LiF, MgF_2, NaCl, NaF, SrF_2, ZnS (CVD), and ZnSe (CVD). The piezo-optic constants of the following materials are presented: As_2S_3 glass, CaF_2, BaF_2, Ge, KCl, fused SiO_2, SrF_2, a chalcogenide glass (Ge 33%, As 12%, Se 55%) and ZnSe (CVD).

17. KEY WORDS *(six to twelve entries; alphabetical order; capitalize only the first letter of the first key word unless a proper name; separated by semicolons)* Al_2O_3; As_2S_3 glass; BaF_2; CaF_2; CdF_2; chalcogenide glass; elastic compliances; elastic constants; elasto-optic constants; fused silica; Ge; hot forged; KBr; KCl; KCl:KI; LiF; MgF_2; NaCl; NaF; piezo-optic constants; refractive index; SiO_2; SrF_2; thermal expansion coefficient; thermo-optic constant; ZnS; ZnSe

18. AVAILABILITY	☒ Unlimited	19. SECURITY CLASS (THIS REPORT)	21. NO. OF PRINTED PAGES
☐ For Official Distribution. Do Not Release to NTIS		UNCLASSIFIED	71
☒ Order From Sup. of Doc., U.S. Government Printing Office, Washington, DC 20402, SD Stock No. SN003-003–02031-1		20. SECURITY CLASS (THIS PAGE)	22. Price $2.40
☐ Order From National Technical Information Service (NTIS), Springfield, VA. 22161		UNCLASSIFIED	

USCOMM-DC

NBS TECHNICAL PUBLICATIONS

PERIODICALS

JOURNAL OF RESEARCH—The Journal of Research of the National Bureau of Standards reports NBS research and development in those disciplines of the physical and engineering sciences in which the Bureau is active. These include physics, chemistry, engineering, mathematics, and computer sciences. Papers cover a broad range of subjects, with major emphasis on measurement methodology, and the basic technology underlying standardization. Also included from time to time are survey articles on topics closely related to the Bureau's technical and scientific programs. As a special service to subscribers each issue contains complete citations to all recent NBS publications in NBS and non-NBS media. Issued six times a year. Annual subscription: domestic $17.00; foreign $21.25. Single copy, $3.00 domestic; $3.75 foreign.

Note: The Journal was formerly published in two sections: Section A "Physics and Chemistry" and Section B "Mathematical Sciences."

DIMENSIONS/NBS

This monthly magazine is published to inform scientists, engineers, businessmen, industry, teachers, students, and consumers of the latest advances in science and technology, with primary emphasis on the work at NBS. The magazine highlights and reviews such issues as energy research, fire protection, building technology, metric conversion, pollution abatement, health and safety, and consumer product performance. In addition, it reports the results of Bureau programs in measurement standards and techniques, properties of matter and materials, engineering standards and services, instrumentation, and automatic data processing.

Annual subscription: Domestic, $11.00; Foreign $13.75

NONPERIODICALS

Monographs—Major contributions to the technical literature on various subjects related to the Bureau's scientific and technical activities.

Handbooks—Recommended codes of engineering and industrial practice (including safety codes) developed in cooperation with interested industries, professional organizations, and regulatory bodies.

Special Publications—Include proceedings of conferences sponsored by NBS, NBS annual reports, and other special publications appropriate to this grouping such as wall charts, pocket cards, and bibliographies.

Applied Mathematics Series—Mathematical tables, manuals, and studies of special interest to physicists, engineers, chemists, biologists, mathematicians, computer programmers, and others engaged in scientific and technical work.

National Standard Reference Data Series—Provides quantitative data on the physical and chemical properties of materials, compiled from the world's literature and critically evaluated. Developed under a world-wide program coordinated by NBS. Program under authority of National Standard Data Act (Public Law 90-396).

NOTE: At present the principal publication outlet for these data is the Journal of Physical and Chemical Reference Data (JPCRD) published quarterly for NBS by the American Chemical Society (ACS) and the American Institute of Physics (AIP). Subscriptions, reprints, and supplements available from ACS, 1155 Sixteenth St. N.W., Wash., D.C. 20056.

Building Science Series—Disseminates technical information developed at the Bureau on building materials, components, systems, and whole structures. The series presents research results, test methods, and performance criteria related to the structural and environmental functions and the durability and safety characteristics of building elements and systems.

Technical Notes—Studies or reports which are complete in themselves but restrictive in their treatment of a subject. Analogous to monographs but not so comprehensive in scope or definitive in treatment of the subject area. Often serve as a vehicle for final reports of work performed at NBS under the sponsorship of other government agencies.

Voluntary Product Standards—Developed under procedures published by the Department of Commerce in Part 10, Title 15, of the Code of Federal Regulations. The purpose of the standards is to establish nationally recognized requirements for products, and to provide all concerned interests with a basis for common understanding of the characteristics of the products. NBS administers this program as a supplement to the activities of the private sector standardizing organizations.

Consumer Information Series—Practical information, based on NBS research and experience, covering areas of interest to the consumer. Easily understandable language and illustrations provide useful background knowledge for shopping in today's technological marketplace.

Order **above** *NBS publications from: Superintendent of Documents, Government Printing Office, Washington, D.C. 20402.*

Order **following** *NBS publications—NBSIR's and FIPS from the National Technical Information Services, Springfield, Va. 22161.*

Federal Information Processing Standards Publications (FIPS PUB)—Publications in this series collectively constitute the Federal Information Processing Standards Register. Register serves as the official source of information in the Federal Government regarding standards issued by NBS pursuant to the Federal Property and Administrative Services Act of 1949 as amended, Public Law 89-306 (79 Stat. 1127), and as implemented by Executive Order 11717 (38 FR 12315, dated May 11, 1973) and Part 6 of Title 15 CFR (Code of Federal Regulations).

NBS Interagency Reports (NBSIR)—A special series of interim or final reports on work performed by NBS for outside sponsors (both government and non-government). In general, initial distribution is handled by the sponsor; public distribution is by the National Technical Information Services (Springfield, Va. 22161) in paper copy or microfiche form.

BIBLIOGRAPHIC SUBSCRIPTION SERVICES

The following current-awareness and literature-survey bibliographies are issued periodically by the Bureau:
Cryogenic Data Center Current Awareness Service. A literature survey issued biweekly. Annual subscription: Domestic, $25.00; Foreign, $30.00.
Liquified Natural Gas. A literature survey issued quarterly. Annual subscription: $20.00.

Superconducting Devices and Materials. A literature survey issued quarterly. Annual subscription: $30.00. Send subscription orders and remittances for the preceding bibliographic services to National Bureau of Standards, Cryogenic Data Center (275.02) Boulder, Colorado 80302.